Politecnico di Milano

School of Civil, Environmental and Land Management Engineering

Master of Science in Hydraulic Engineering

Master's Degree Thesis

Hydrological modelling of flood forecasting of the Medellín river in Colombia

Supervisor
Giovanni RAVAZZANI

Assistant supervisor
Lisdey Verónica HERRERA GÓMEZ

Author
Sofia TERBISI (899881)

A.Y. 2020/2021

Abstract

The aim of this thesis is the application of a hydrological model to ameliorate the flood forecasting system of Aburrá valley's metropolitan area in Colombia. Currently, the warning system is based on the observation and is subject to exceeding the threshold water levels of the Medellín river, the alert is given only some hours before an event. The application of a hydrological model coupled with a meteorological one, would mean an important advance in alerting the responsible bodies and consequently allowing the securing of people and goods with greater efficacy.

The hydrological model applied is the *Flash-flood Event-based Spatially- distributed rainfall-runoff Transformation - Water Balance (FEST-WB)*, largely employed for the study of the hydrological water balance and flood forecasting of alpine basins. The objective is to evaluate whether this model is also applicable to basins with climatic and morphological features which differ from the usual field of application. The input employed is composed by meteorological and hydrological data measured by the *Sistema de Alerta Temprana de Medellín y el Valle de Aburrá (SIATA)*. Subsequently, in order to define the flood forecasting capacity of the model, the data from the *Global Forecast System (GFS, NOAA/NCEP, USA)* models are used.

Although this work is a preliminary study, the hydrological model proves to be adaptable to this kind of basin, and, therefore, employable for the flood forecasting and alert system in the examined area which is often prone to hydraulic risks.

Key words: flood forecasting; hydrological model; FEST; warning system; Medellín; Colombia.

Sommario

La presente tesi si propone di applicare un modello idrologico per migliorare il sistema di allertamento delle piene nell'area metropolitana della valle di Aburrá in Colombia. Attualmente, l'allerta viene data solo poche ore prima di un evento. Il sistema si basa su delle osservazioni, viene monitorato il livello fluviale del fiume Medellín e in caso di superamento di una soglia viene dato l'allarme. L'applicazione di un modello idrologico, accoppiato ad uno meteorologico, permetterebbe di allertare gli enti preposti con sufficiente anticipo, consentendo la messa in sicurezza della popolazione e dei beni con maggiore efficacia.

Il modello idrologico applicato è il *Flash-flood Event-based Spatially- distributed rainfall-runoff Transformation - Water Balance (FEST-WB)*, largamente impiegato nei bacini alpini per lo studio del bilancio idrologico e per la previsione delle piene. Si vuole valutare se tale modello è applicabile anche in bacini con caratteristiche climatiche e morfologiche differenti dal consueto campo di applicazione. Gli input utilizzati sono dati meteorologici ed idrologici misurati sul campo dal *Sistema de Alerta Temprana de Medellín y el Valle de Aburrá (SIATA)*. Successivamente, per definire la capacità di predizione delle piene, vengono impiegati i dati provenienti dal modello meteorologico *Global Forecast System (GFS, NOAA/NCEP, USA)*.

Nonostante questo lavoro rappresenti un'analisi preliminare, il modello idrologico risulta adattabile a questo tipo di bacino e quindi utilizzabile per l'allertamento e la previsione delle piene nell'area in esame che spesso è soggetta a rischi idraulici.

Parole chiave: previsione delle inondazioni; modello idrologico; FEST; sistema di allerta; Medellín; Colombia.

List of Figures

List of Tables

Contents

Chapter 1

Introduction

The several flood events registered in Colombia and, above all, the high quantity of damage to people and goods that these events caused, underlined the weakness in the approach to managing flood risks in the country. These events have also a negative effect on the economy and the ecology of Colombia. Indeed, every year the heavy rains lead to flooding of rivers and, consequently, landslides that cause dozens of deaths and thousands of displaced. Specifically from early March to the end of June of 2021, which corresponds approximatively to the first rainy season of the year, 74 deaths, 54 injured and 7 missing were reported. This was a consequence of the 1154 rainfall events occurred in 515 municipalities of the State [2]. In figure 1.1 are shown significant photos of the events of this period.

Currently, in Colombia, a uniformed flood forecasting system does not exist. Although a few warning schemes had been developed in selected basins by communities and local authorities, often these systems do not manage to give the warning in time. The present situation in Colombia is more or less the same as the one of the neighbouring countries. The biggest issue is the lack of a national authority that can coordinate and manage the implementation of the forecast model [3]. The meteorological condition of South-America complicates the situation because of its unpredictability, worsened to climate change.

This thesis has the aim to understand if there is the possibility to apply a model of flood forecast in a specific basin of Colombia and then eventually applying the system to other basins. Indeed, the risk given by the flood can be reduced thanks to the prediction of the event. This can reduce the part of the risk linked to the exposed elements and their vulnerability. A long term prediction of an overflow allows the responsible bodies to secure people and properties. It is fundamental to remind that the action of prediction of the critical events does not mean the elimination of the event but can be useful for the management of it.

The area of study is the Aburrá valley in Antioquia department, it is the natural

(a) Flood in Santa Rosa de Osos - 15/06/2021 Photo: Dagran. [2]

(b) Flood in a street of Medellín - 11/06/2021 Photo: Cortesía Denuncias Antioquia y Alcaldía de Medellín . [2]

Figure 1.1: Examples of the effects of a flood during June 2021 in Antioquia

basin of river Medellín. The focus is on the Medellín city, the second-largest city of Colombia after Bogotá. The high level of urbanization caused frequent and dangerous floods. For this reason, the municipality of Medellín together with the public company EPM and the private one ISAGEN developed the Aburrá valley early warning system (SIATA) [1]. The aim of this system is to predict a natural event that can modify the environmental conditions of the area or that can be dangerous for the population. This operation is done starting from a solid real-time monitoring network.

A hydrological model can be applied in the basin thanks to the high number of spatial and temporal data. In this paper, the hydrological model used is the one called FEST-WB (Flash - flood Event - based Spatially distributed rainfall - runoff Transformation - Water Balance). FEST is a distributed model widely used in Italy; it gives an hydrogram knowing the rainfall and some descriptive parameters of the basin.

1.1 Literature review

River flooding currently impacts more people than any other environ-mental event posing a threat to almost 380 million urban residents globally [4]. During the last decades, extreme events have occurred with higher frequency due to climate change [5]. By combining this effect with the population growth and rapid urbanization, some countries will be more exposed to flood risk. Flood forecast event is central in the management of river flooding.

(Jain et al., 2018 [6]) present different aspect of flood forecasting and give a classification of model used for flood forecasting. The main subdivision is between stochastic and deterministic model. The first type simulate the random and probabilistic nature of inputs and responses that govern river flow. Deterministic models solve a set of equation representing the different watershed processes. These type of models can be classify according to the spatial distribution of inputs and parameters. In lumped models, the catchment is idealized with various storage tanks, modelling consists in describe the movement of water through these tanks. In contrast, in a distributed model the catchment is divided into a large number of cells. Another important category is the model that use the concept of ensemble forecasting. The ensemble prediction systems offers an ensemble prediction of hydrological variables. This result is obtained through small changes in the initial conditions, different representations of the physical processes and changes in parametrization and solution schemes.

(Alfieri et al., 2013 [7]) presents the Global Flood Awareness System (GloFAS), it is based on distributed hydrological simulation of numerical ensemble weather prediction with global coverage. Streamflow forecasts are compared statistically

to climatological simulations to detect probabilistic exceedance of warning thresholds. River discharge is simulated by the Lisflood hydrological model for the flow routing in the river network and groundwater mass balance. Lisflood is a GIS-based spatially distributed hydrological model, which include a one-dimensional channel routing model (van der Knijff et al., 2010 [8]). The Lisflood model is currently running within the European Flood Alert System (EFAS).

(Thielen er al., 2009 [9]) presents the European Flood Alert System in which the ensemble of multiple hydrographs is analysed and combined to produce early flood warning information. EFAS is part of strategy for improved disaster management in Europe to reduce the impact f transnational floods through early warning. This can be achieved by providing National hydrological services with early flood information in addition to their own local and, mostly often, short-range forecasting information.

Flash floods are a recurrent hazard for many developing Latin American regions due to their complex mountainous terrain and the rainfall characteristics in the tropics [1].

(Domínguez-Calle and Lozano-Báez, 2014 [10]) does a review of the literature on the early warning systems for floods and droughts. It also present early warning systems in Colombia. Event of La Niña in 2010 and 2011 caused economic loss, damage at the infrastructure and human losses, events of this size underlined lacks in the risk management and the necessity of early warning system in Colombia. The first system for risk management in Colombia was created in 1989 and was the SNGRD (Sistema Nacional de Gestión del Riesgo de Desastres). The first experience of the warning system was in 1976 thorough the SCMH (Servicio Colombiano de Hidrologia y Meteorología). Currently the IDEAM (Instituto de Hidrologia, Meteorologia y Estudios Amebientales) presents a daily report of the hydrological warning and generates a public announcement for extraordinary events. This forecast system is based on the Water Research and Forecasting model (WRF) and on the V5 (MM5) model. Both the models use as initial conditions the data of the Global Forecast System (GFS, NOAA/NCEP, USA)

(López-García et al.,2015 [11]) review approaches to and field experiences with EWS (Early Warning System) throughout the world, including Colombia. They identified that many EWS are unimplemented; and once in operation, there exist an imbalance among ocmponents. On the other hand, some EWS fail to meet the territory need as a result of poor community participation, both at design and operation stages.

(Ochoa Isaza, 2013 [12]) analyses the hydrological distributed model (SHIA) on the Medellín river in the Aburrá valley. This study is done with the aim of evaluated the impact of information that come from radar on the simulation. The distributed model SHIA is currently use in the early warning systems of Medellín

in the Aburrá valley (SIATA).

1.2 Structure of the thesis

Chapter 2 presents the study area with a geographical, morphological and climatic overview useful to understand the context in which the basin is inserted. Informations about land cover and soil texture are also reported. At the end of the chapter there is a description of the data network present in the Aburrá valley with a focus on the part used in this work.

In chapter 3 is presented the hydrological model, the main equation used by the model are reported. In it's section 3.3 there is the application of the model and the results.

In chapter 4 the hydrological model is coupled with a global meteorological model. Hydrological model is applied with forecast inputs at two different periods in which flood of river Mdellín are registered.

In the last chapter (chapter 5) there are the discussion of the results and the future developments.

Chapter 2

Study area

This chapter presents the basin under study. The main characteristics are reported, focusing attention on those that most influence the hydrological response of the basin. The information reported is the one of interest for the model and for the equations that are applied. The last part of the chapter describes the data network present in the basin.

2.1 Geographical and morphological overview

The area under consideration is the Aburrá Valley, in which is located the second biggest urban agglomeration of Colombia, for both population and economy. This valley is in the Antioquia Department, in the North West of Colombia (figure 2.1). The Aburrá Valley is located in the middle of Central Andes, therefore the territory is mountainous with irregular topography. Altitude is between 1300 and 2800 m a.s.l., the slope varies between 1-25% in 40% of the territory, 45% of the area has slightly steep terrain with slopes between 25-50% and the remaining 15% is steep with slopes that exceed 50%. The Digital Elevation Model is reported in figure 2.2, the dimensions of the cell are 200x200 metres. The urbanized area of the valley is the Metropolitan Area of the Aburrá Valley and rises in the flat area near the main river.

The valley understudy constitutes the natural basin of the river Medellín which runs from South to North for 100 km. The watershed has an elongated shape in the north-east direction. The Medellín river originates in the south part of the basin, in the small town called Caldas, more specifically in the Alto de San Miguel at 2800 meters above sea level. The river runs through the entire valley to the limit of Barbosa town where it flows, together with the Rio Grande, into the Porce. In figure 2.2 the hydrographic network and the main reach can be seen. Medellín river is the main one, it cuts through the valley, the others rivers are all its

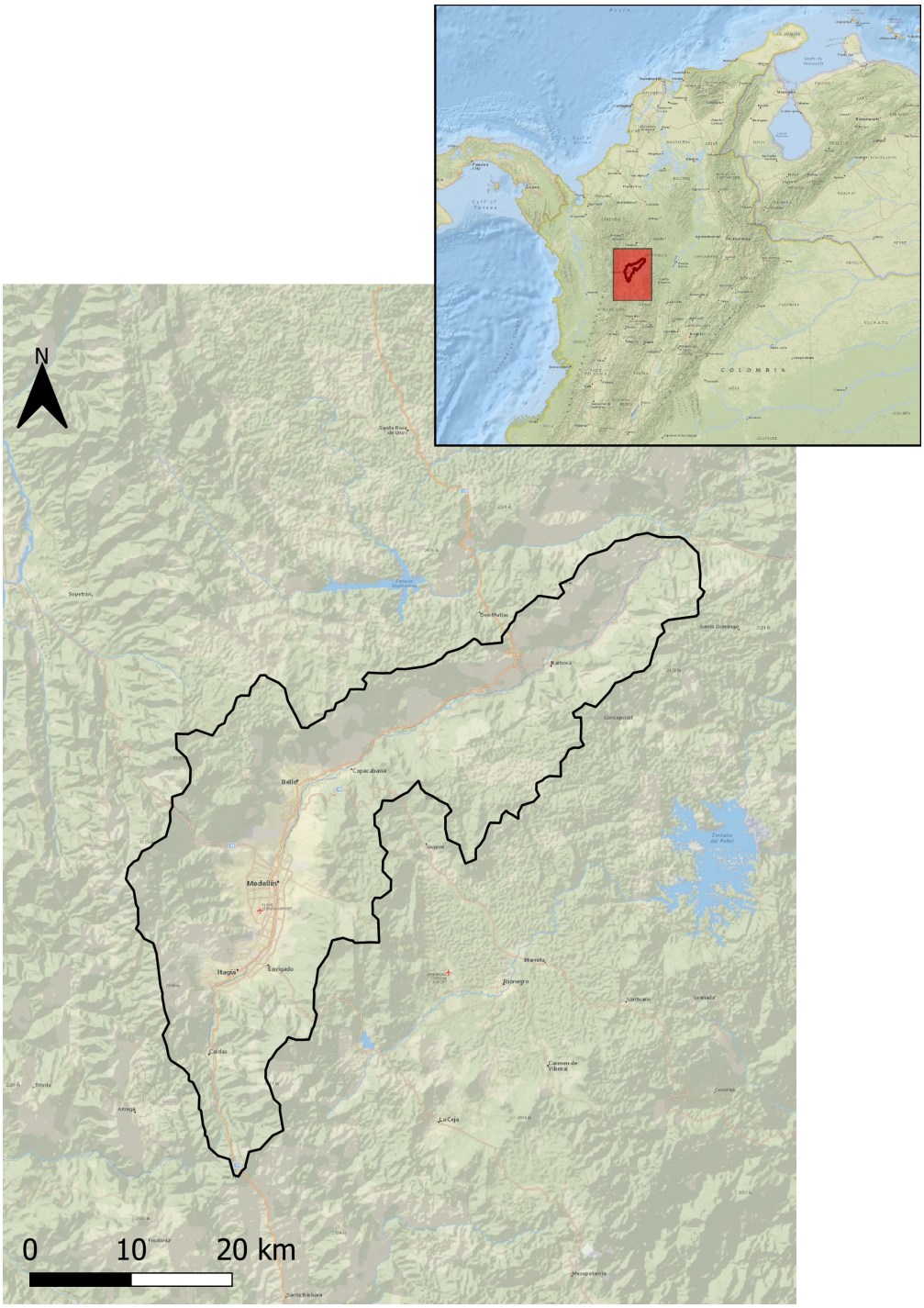

Figure 2.1: Geographic context

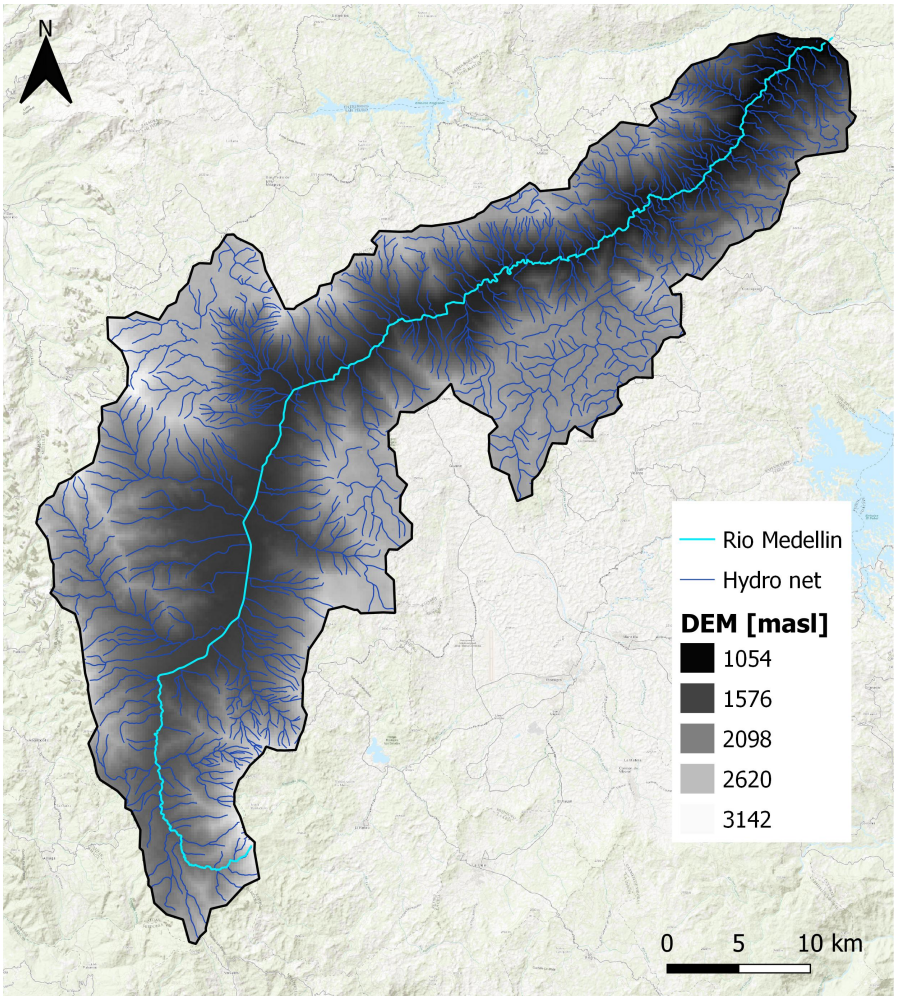

Figure 2.2: Digital Elevation Model and hydrographic network

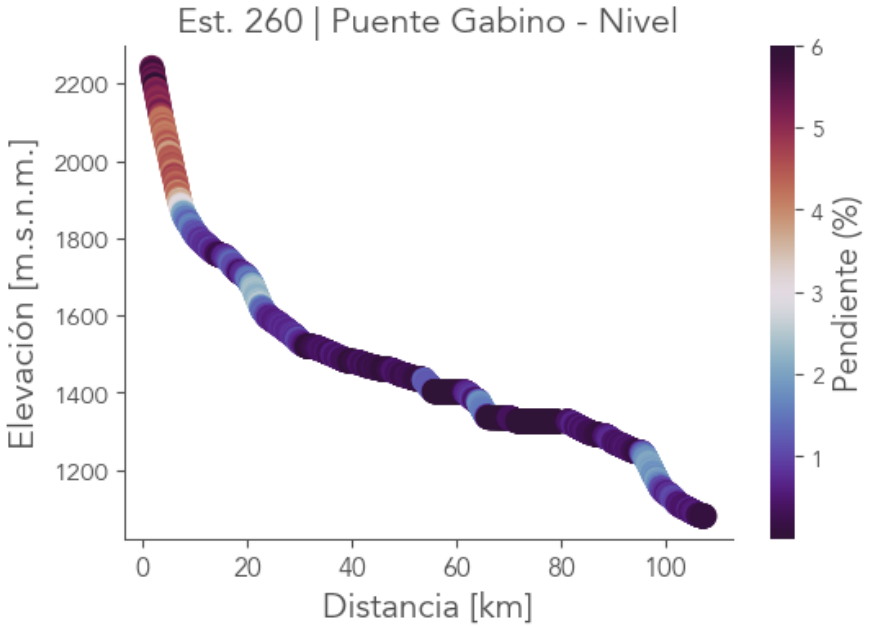

Figure 2.3: Medellín's river elevation profile

tributaries [12]. The hydrographic network reported comes from digitalization of physics maps. In figure 2.3 is reported the altitude profile of the river Medellín [1]. Some feature of the watershed are reported in table 2.1.

Along the main reach, there is only one deviation of the discharge. At the end of the river, between the municipalities of Barbosa and Santo Domingo, there is the hydroelectric power plant, Central Hidroeléctrica Carlos Lleras Restrep, it takes the waters through a spillway but it puts it back in the river. An additional discharge on the river, also located in the municipality of Barbosa, comes from La Tasajera hydroelectric power plant, which contributes, at most, with 40 m^3/s; so, at the very end of the basin the discharge of Medellín includes also this value coming from another basin. Therefore all the rainwater, that doesn't evaporate or filtrate deeply, joins the closing section of the basin. In general, the basin has a good capacity to keep the discharge, with a high and very high WRI (Water Retention Index) [13].

Area [km²]	1'218
Mean altitude [m.a.s.m]	1996
Basin mean slope [%]	22
Main channel mean slope [%]	0.72
Main channel [km]	107.67

Table 2.1: Basin's morphological characteristics

2.2 Land cover

The territory analysed is located in the central Andes, has a latitude of 6 degrees north and reaches altitude of 2800 meters above sea level. These properties ensure that the basin is entirely covered by vegetation and the exclusion of the urban area that develops around the Medellin river. Figure 2.4 shows the land cover map produced by the ISCGM[1] [14]. The Global Land Cover by National Mapping Organizations classifies the status of the land cover into 20 categories. The classification is based on Land Cover Classification System (LCCS) developed by FAO. In the Aburrá valley, the non-urban areas are divided between forests and cultivated fields. The latter (in yellow in figure 2.4) is mostly located in the flattest areas of the basin and in its terminal part.

2.3 Soil texture

To study the flow is created in the basin it is necessary to know some descriptive parameters of the soil. These are related to the texture of the soil, in fact, they are derived from empirical expressions knowing the type of soil.

Information about soil texture is available on the SoilGrids portal, a system for digital soil mapping based on a global compilation of soil profile data (WoSIS[2]) and environmental layers [15]. In figure 2.5, 2.6 and 2.7 are shown maps with the content of, respectively, clay, sand and silt at depth equal to 5/15 cm, the white parts are the urbanized area. The mean values of the three percentages are reported in table 2.2. Looking at these maps, it is possible to say that, in the entire basin there is the same texture. For this cause is reasonable to assume that, also under the urban area, there is the same soil texture.

Knowing percentages of silt, sand and clay is possible to obtain the soil type thanks to the USDA soil textural triangle (figure 2.8), this is the most simple and common way to classify soil [16]. The type of soil identify through the graph of the USDA classification, using the mean value of percentages of the content of sand,

[1] International Steering Committee for Global Mapping
[2] World Soil Information Service

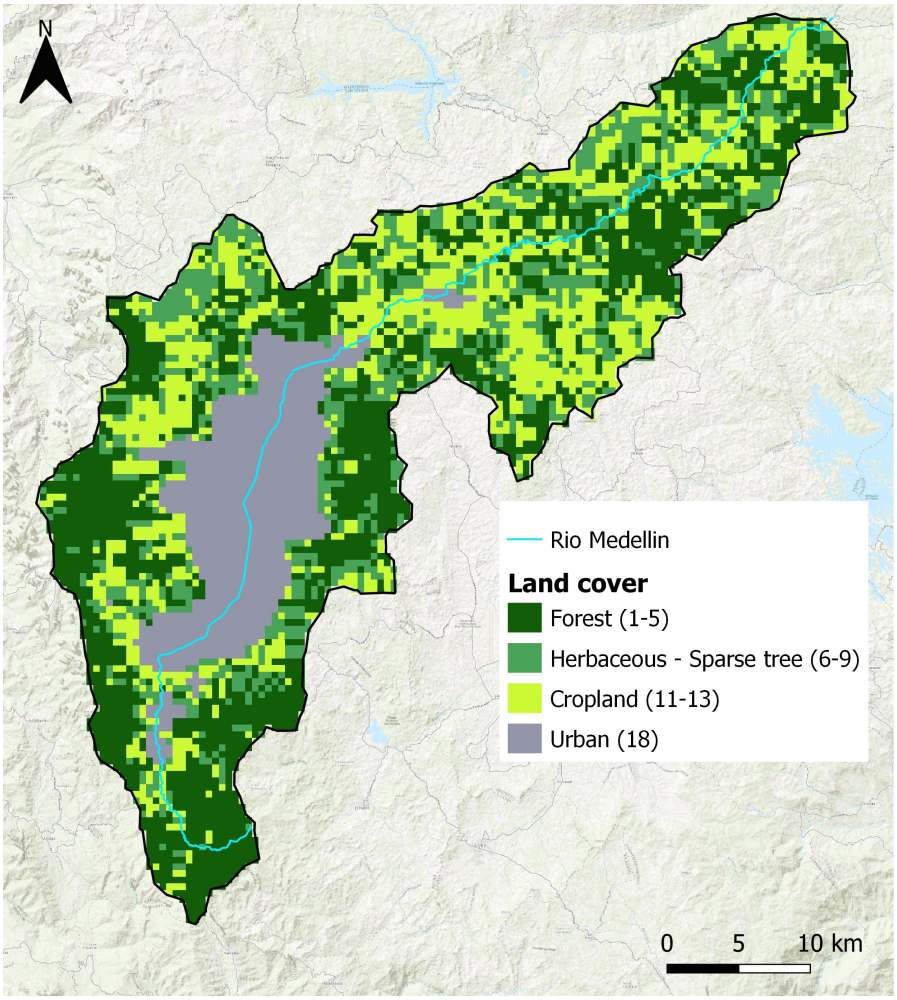

Figure 2.4: Land cover map by ISCGM

silt and clay, is *Clay Loam*. This soil, in general, has the characteristics of clay but, in this case, the presence of silt and sand mitigate its features. Loams that contains clay tends to be heavy because of the density of clay. The density of the clay is the cause of the two biggest drawbacks of clay loam. When it is very wet, it swells to retains water, on the other hand, dry clay shrinks but stays packed, forming dense clods and cracking the soil surface.

	Mean content	
	[g/kg]	%
Clay	271.7	27.2
Sand	296.5	29.7
Silt	280.6	28.1

Table 2.2: Mean value of soil content

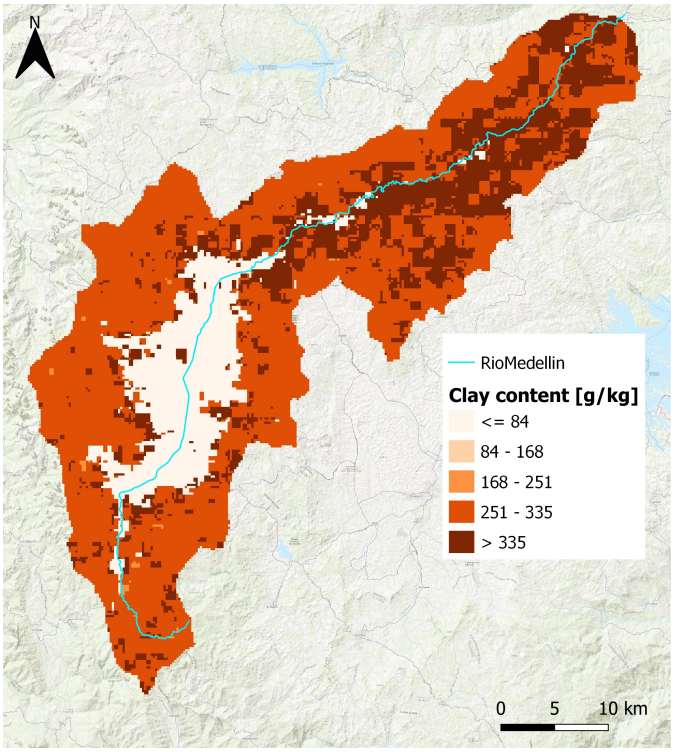

Figure 2.5: Soil clay content

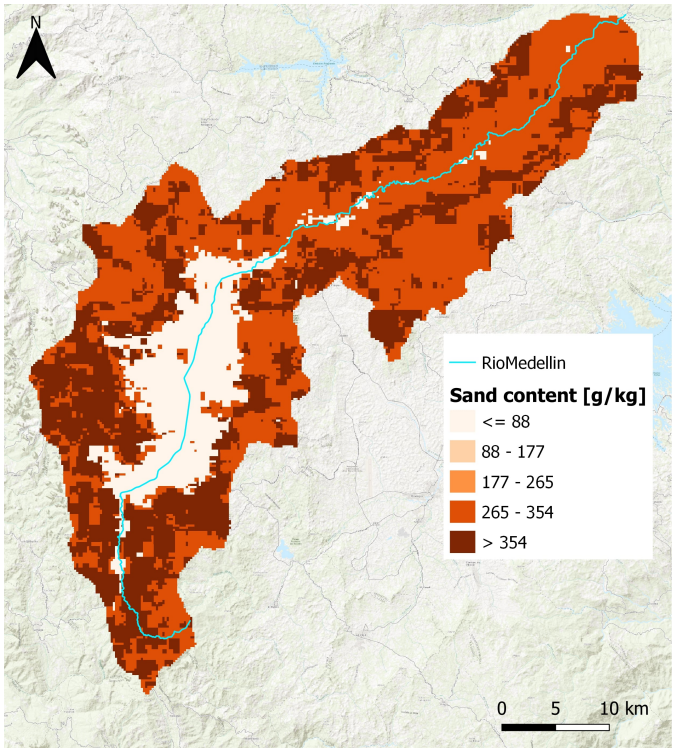

Figure 2.6: Soil sand content

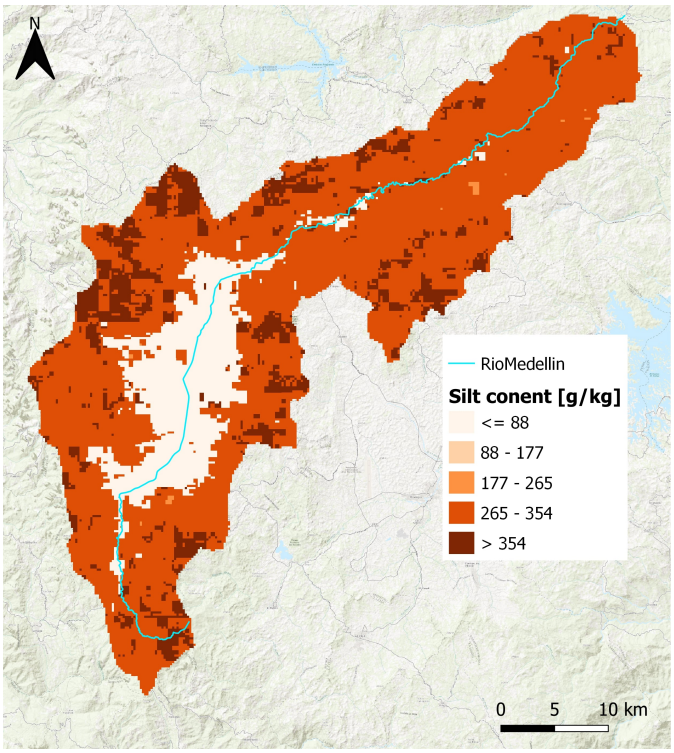

Figure 2.7: Soil silt content

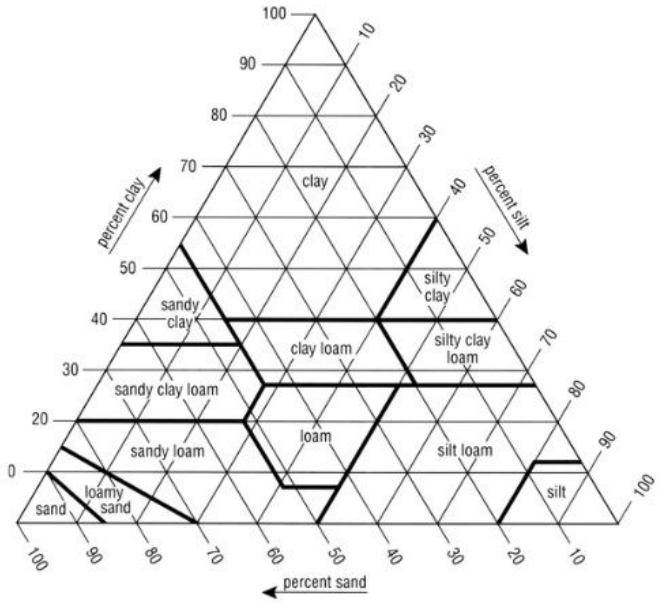

Figure 2.8: USDA Soil textural triangle

2.4 Climatic context

The study area is classified, according to the Kröppen climate classification, as a tropical monsoon climate in the version of a less pronounced dry season. This means a climate almost uniform year-round. Thanks to the altitude of the valley, its climate is not as hot as other cities in the same latitude near the equator. The variation of temperature is limited, over the year there is about a constant temperature equal to 15/20°C. Albeit it's possible to identify two rainy seasons, there isn't a real dry season, rains are registers all over the year. The rainy intervals are March-April-May and September-October-November, these periods are characterized by a copious amount of rain usually in the form of frequent thunderstorms [12]. The mean precipitation changes with the altitude, in Medellín it can reach the values of 2630 $mm/year$ [17]. Often the events are short but of high intensity and they are localized in a confined area. Since there are frequent rains when an event occurs the soil is already almost saturated so, the problem is to drain the rainwater. Photos in figure 2.9 are an example of the type of rainfall events in Medellín [18].

2.5 Data network

The watershed under study has a rich data network thanks to the system of early warning of Medellín and the Aburrá valley (SIATA). This system was established by the municipality of Medellín together with company EPM and ISAGEN. The main objectives of the project are real-time monitoring and early alerts. The network was activated in 2010 starting with 16 rainfall stations that measured the millimetres of precipitation with an interval of five minutes. Over the years it has developed by measuring different types of parameters both with remote sensing and with sensors located on the territory. Since 2013, the time interval has been reduced to one minute.

As a part of this thesis a small part of the monitoring network was used, specifically, the meteorological and the hydrological ones. The meteorological network includes sensors for measuring precipitation, temperature, pressure, wind speed, humidity and solar radiation. For the application of the hydrological model FEST, only precipitation and temperature data were collected. That is because measures of other quantities are too recent, so they don't provide a sufficient amount of data to do the hydrological simulation. The hydrological network measures the surface velocity and the water height of watercourses. These measurements are combined with the survey of the cross sections where the sensors are placed. [1]

(a) Medellín, 05 April 2021 [19]

(b) Medellín, 24 December 2020 [20]

Figure 2.9: Photos of rainfall events in Medellín

Meteorological network

Rainfall is measure principally through pluviometers, that produce a value in mm of the depth of the precipitation that occurs over an unit of area in one minute. Other sensors to measure rain are disdrometers and meteorological sensors. The first one gives the amount of rainfall through measures of diameter and velocity of drops. The second type of sensor is a multiparametric one that provides information about precipitation, temperature, relative humidity, atmospheric pressure and wind velocity and direction.

On the territory the total amount of stations that can register precipitation is 224. However, some of them were not considered in this paper because they are too far from the basin under study or are activated only from a few months. The location of the 167 sensors take into account is shown in figure 2.10a. Some of the station examined are out of the basin but they are useful to recreate the precipitation in the area with only few sensors.

The same observation is valid for the temperature stations, in this case the total amount of sensors is 44 but only 24 are been considered. The location of the stations take analysed is reported in 2.10b. The scale color of the sensors in figure 2.10 depends on the date of activation, the lighter ones have been in operation for less time.

Hydrological network

From hydrological network were used sensors for the measurement of water depth and velocity. These two quantities are useful to calculate the discharge. In each station taken into account is important that, for at least a period of time, are present measures of both water depth and velocity. The instruments are electromagnetic and measure the distance from the free surface. Some instruments use electromagnetic waves while others use ultrasonic. The position of the stations for the water depth measure are strategical because some of them are monitored for the early alert. Sound alarms are activated when the free surface reaches a certain level. This system allows the risk management stakeholders to evacuate the community. Albeit the network for the measurement of the water depth is very rich (88 stations), only 19 stations measure also the superficial velocity of the rivers and which 7 of the velocity stations have a significant amount of data since were installed before 2019. As it's shown in figure 2.11, five stations are on the main channel of the basin, Medellín river, and the remaining two stations are located on two different tributaries of Medellín.

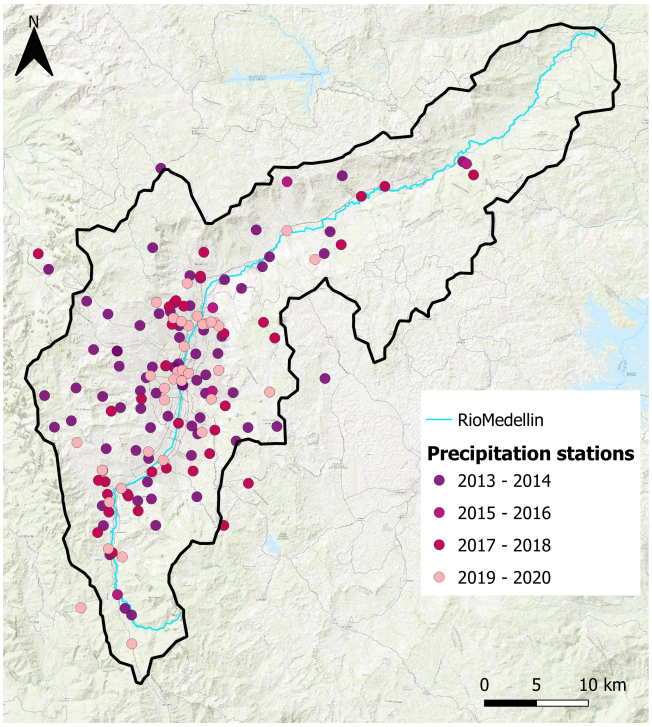

(a) Precipitation measurement stations

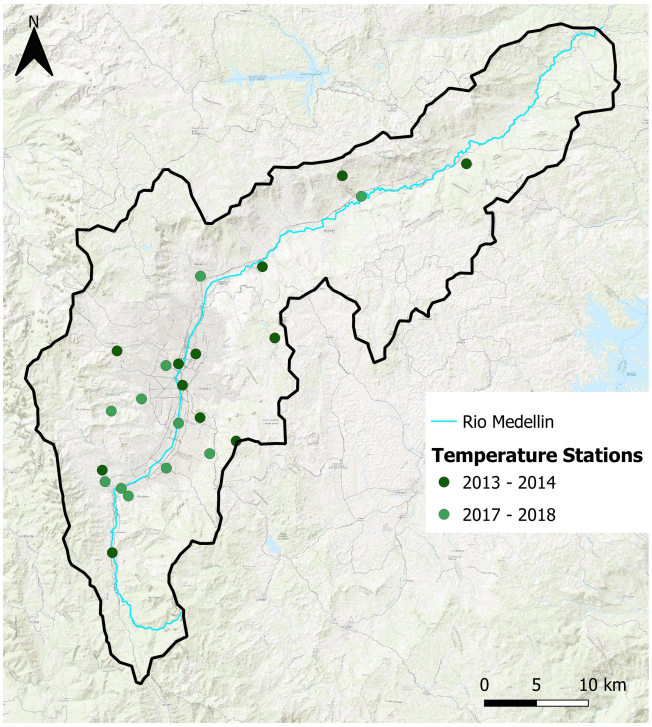

(b) Temperature measurement stations

Figure 2.10: Meteorological stations

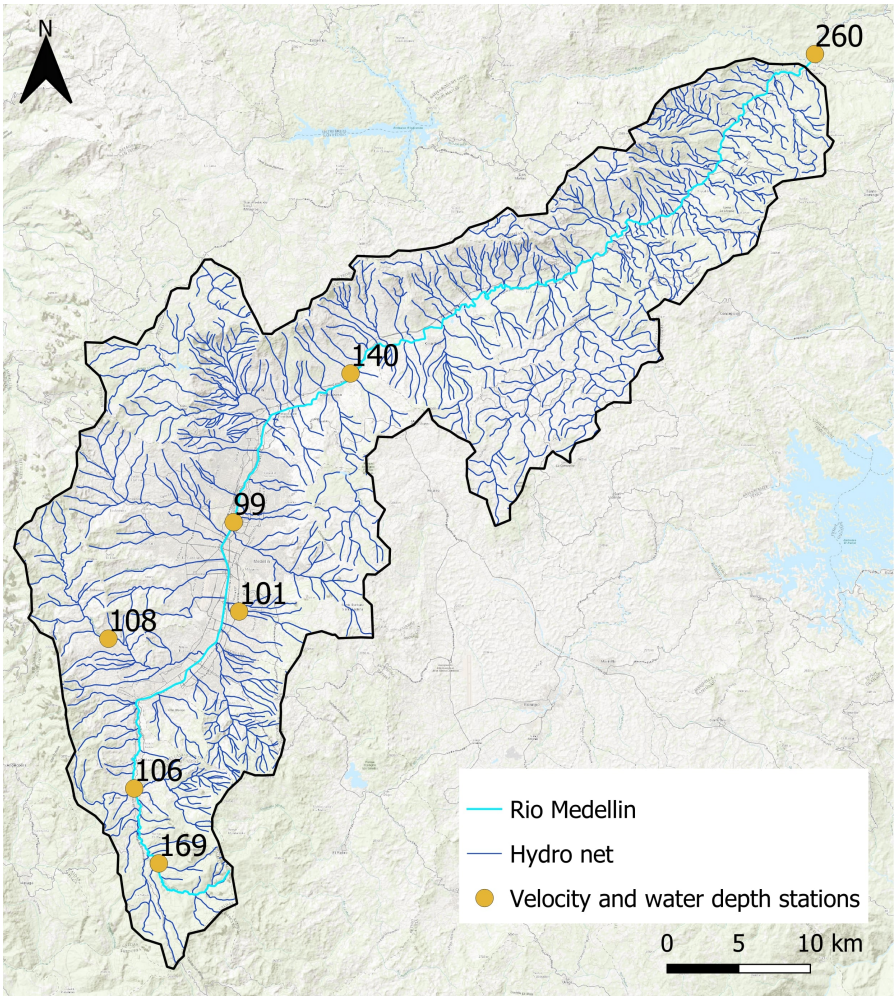

Figure 2.11: Velocity and water depth stations

Chapter 3

Hydrological model

In this work the hydrological simulations are done with the model FEST-WB (Flash-flood Event-based Spatially-distributed rainfall-runoff Transformation - Water Balance) [21] [22] [23], a distributed hydrological continuous water balance model developed on the event based model FEST. Starting from the atmospheric forcing and soil parameters FEST-WB computes the outflow hydrograph through a water balance that considers the main processes of the hydrological cycle: evapotranspiration, infiltration, surface runoff, subsurface flow and snow dynamics (figure 3.1). In figure 3.2 there is a diagram of the model [24].

The FEST-WB model is classified as a distributed physic-based model. A physical based model is the one that applies the water balance considering the real hydrological dynamics and physical parameters that describe the basin. Distributed means that the spatial variation of the physical parameters, which describe the basin, is considered and therefore the computational domain is discretized with a mesh of regular square cells in each of which the water balance is calculated. Indeed, the value of the parameters and input data are given as a grid, value for each cell. Spatial variability is better considered with a more fine discretization, this, however, increases the calculation time.

3.1 Input data

The inputs of the model are meteorological forcing and grid maps of elevation and soil parameters.

The meteorological data depends on the equations used in the model, for this work the chosen formulas require only precipitation and temperature as input. The two variables are available in the portal of SIATA [1], in which the data is published every month. These data have been elaborated to create the input of the model. It consists of a file in which are assembled other files for every month

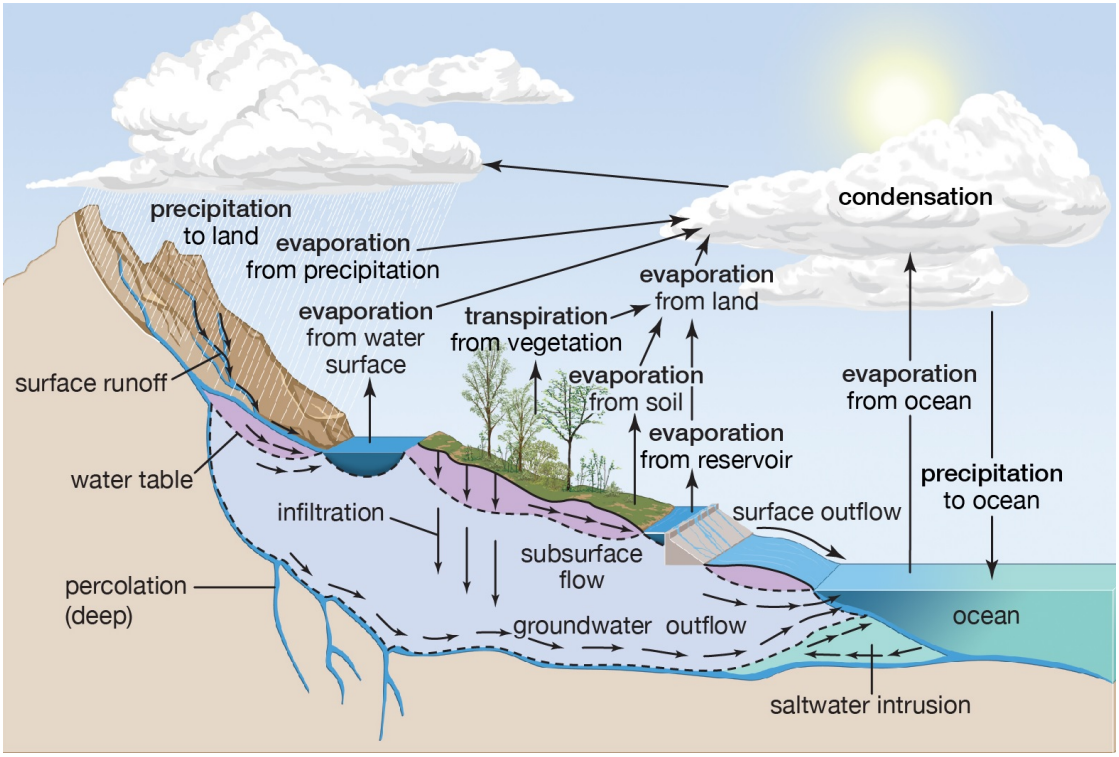

Figure 3.1: Hydrological cycle

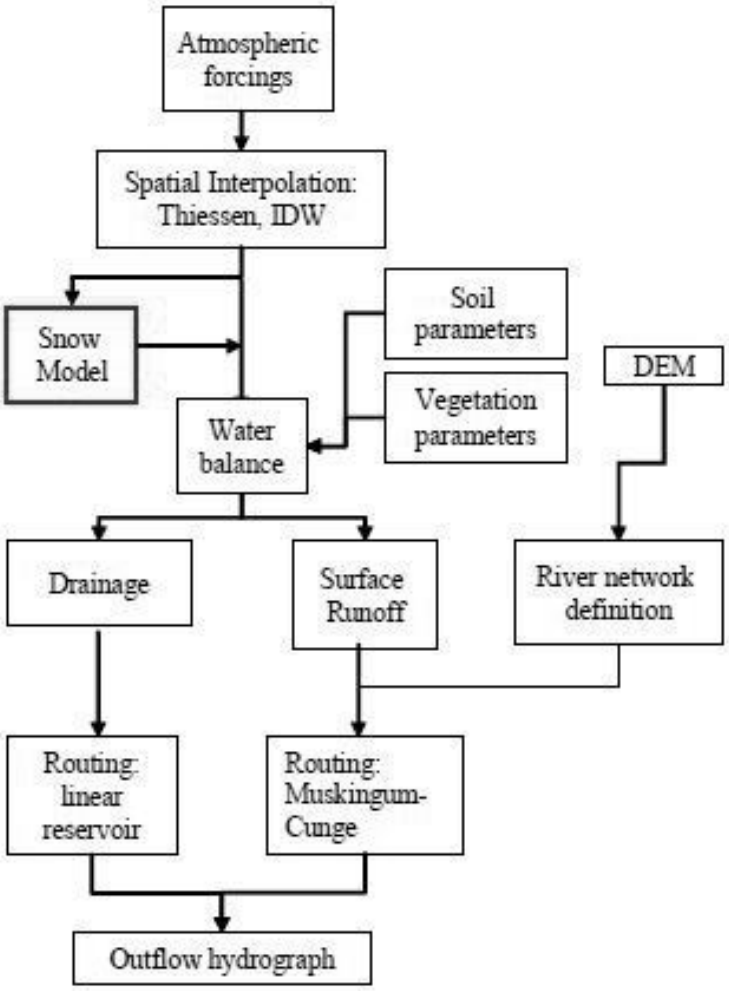

Figure 3.2: Scheme of the hydrological model FEST-WB

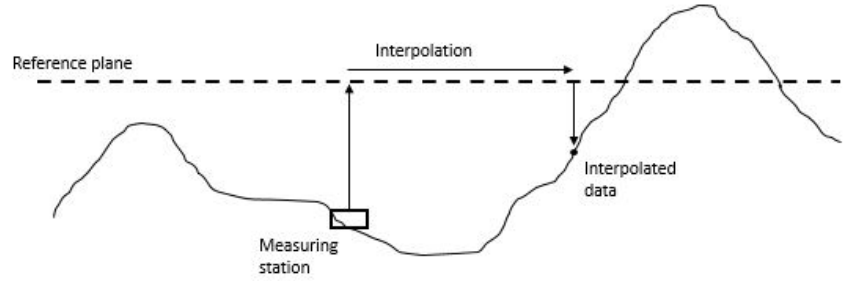

Figure 3.3: Elaboration of temperature data

from 2013 to 2020 and for every station. These data are punctual and stations haven't the same date of installation (figure 2.10). The model applies interpolation to find a value for each cell of the basin from January 2013 to December 2020, of course, the interpolation is more accurate where there is a high concentration of old station. Measures are interpolated using the inverse distance weighting algorithm (IDW). Furthermore, the temperature changes also with altitude so it needs another interpolation. In the model a constant lapse rate adjusts the temperature for elevation, the average thermal gradient applied is $-0.0065\ °C/m$. Operations on temperature consist to scale the measured data into a reference plane with constant altitude, interpolate the date with IDW on this plane and then bring the interpolated date on the ground, in figure 3.3 is described this process. Thermal inversion phenomena are neglected. The results are two maps of cells 200x200 metres with an interpolated value in each cells.

Digital Elevation Model (DEM) is an essential input for the model, in each cell of this map is reported the mean altitude of the cell. The map with the flow path network is automatically derived from the DEM, the procedure consists in assigning flow from each pixel to one of its eight neighbours. From the DEM are also obtain the hillslope and the channel network; the method to do this is to select a constant critical support area that defines the minimum drainage necessary to initiate a channel. The model, in this way, defines two types of cell, channel cells that drain an area greater than the critical one and other cells. Maps with descriptive parameters of the soil are also required. In this case of study, these features are inferred from the type of soil that is the same throughout basin (section 2.3). The input is therefore a map with values from which it is possible to identify the type of soil and, consequently, the descriptive parameters. This map contains the same value for each cells. The parameters used to describe the soil are the following:

- saturated conductivity ($k_{sat}\ [m/s]$)
- saturated and residual volumetric water content ($\theta_{sat},\ \theta_r\ [m^3/m^3]$)

- Brooks and Corey pore size distribution index (B [−]) and tortuosity index [-]
- bubbling pressure [m]
- field capacity and wilting point ($\theta_{lim},\ \theta_{wp}$ [m^3/m^3])
- wetting front soil suction head [m]
- shape parameters of the retention function
- initial abstraction and curve number value
- storativity [mm] and maximum soil storage [m]

3.2 Water Balance

The FEST-WB model solves the water balance equation. Soil moisture (θ) evolution for the generic cell[1] at position i,j is described by water balance equation [22]:

$$\frac{\partial \theta_{i,j}}{\partial t} = \frac{1}{Z_{i,j}} \left(P_{i,j} - R_{i,j} - D_{i,j} - ET_{i,j} \right) \tag{3.1}$$

where P is precipitation rate, R is surface runoff flux, D is drainage flux, ET is evapo-transpiration rate and Z is the soil depth. The quantity $(P_{i,j} - R_{i,j})$ is equivalent to infiltration $I_{i,j}$. The equation (3.1) is solved in the active layer of the basin that need to be set in the model. Under this tier is consider the presence of an impermeable layer.

The next paragraphs describe the physical process and the equations that regulate the water balance.

Drainage flux

The drainage or percolation flux (D) is the vertical flux in the soil. This quantity can be calculated, for one cell of the domain, with the following equation [25]:

$$D_t = k_{sat} \left(\frac{\theta_t - \theta_r}{\theta_{sat} - \theta_r} \right)^{\frac{2+3B}{B}} \tag{3.2}$$

[1] Actually, the equation is applied only in the cell not covered by snow but, in this work, the snow dynamics isn't treat because in the basin snow doesn't exist. For more detail about snow dynamics see [22].

whereas k_{sat} is the vertical permeability of the saturated soil and B is the Brooks and Corey pore size distribution index. The term in brackets is called Θ and is the normalized volumetric water content; it depends on saturated and residual volumetric water content (respectively θ_{sat}, θ_r) and on the water content at time t (θ_t) [26].

Infiltration

The infiltration process refers to the water not intercepted by vegetation for example. The process ends when the rain rate exceeds the infiltration capacity of the soil (Hortonian runoff). There are several models that can describe this process: in the FEST-WB the most used is the SCS-CN method. However, in this work is used the Philip's model, according to Sovinco's thesis in which it emerges as the best among the other ones [27].

Philip's two-term model equation is an approximate solution of Richards' equation for a short infiltration time [28]. The limitation of this approximation is that it can only be applied to homogeneous soil with stagnant initial water content. This is because this model assumes that infiltration starts when there is a layer of water on the ground [29]. According to the Philip's model, cumulative infiltration (I $[L]$) is expressed as:

$$I(t) = St^{1/2} + k_{sat}t \tag{3.3}$$

where S $[LT^{1/2}]$ is the sorptivity and k_{sat} $[LT^{-1}]$ is the saturated hydraulic conductivity. Sorptivity is a physical quantity that measures the capacity of a porous medium to uptake or release water by capillarity. For this reason, the first term of the equation (3.3) dominates the process during the initial stage of infiltration. As infiltration proceeds, the soil begins to get saturated and the second term becomes progressively more important, in this phase the gravitation forces dominate the capillarity. [30]

The rate of infiltration is determined by differential equation (3.3):

$$\frac{dI}{dt} = \frac{1}{2}St^{-1/2} + k_{sat} \tag{3.4}$$

Evapo-Transpiration

Evapo-Transpiration (ET) is the exchange of mass and energy between the soil-water-vegetation system and the atmosphere. ET is the combination of two processes whereby water is lost from the soil surface (E) and from the crop (T).

Evaporation is the process in which liquid water is converted to water vapour and is removed from the evaporating surface. This surface can be, for example,

lakes, soil, pavements and wet vegetation. Transpiration consists in the vaporization of liquid water contained in plant tissues. The water is taken up from the aquifer by the roots and transported through the plant, then the vapour exchange with the atmosphere occurs on the leaves. The requirement energy is given by solar radiation and, to a lesser extent, by the air temperature. The driving force to remove water from surfaces is the difference between the water vapour pressure at the evaporating surface and the one of the atmosphere. The process slows down and stops as the air gradually becomes saturated. It's necessary to replace the humid air with drier air, this process is made possible by the wind. Hence, solar radiation, air temperature, air humidity and wind speed are important parameters in the evaporation process. In this work, however, due to lack of data, it is impossible to use these parameters. For this reason it is applied the Hargreaves and Samani equation in which the inputs are only minimum and maximum air temperature [31] [32].

The real evapo-transpiration is computed by the potential evapo-transpiration (ET_P). It is the maximum quantity of water that can evaporate in the ideal condition, that is, in the state of infinite availability water. In reality, the soil has a humidity condition that limits evapo-transpiration.

Hargreaves and Samani formulation for potential evapo-transpiration is:

$$ET_{pot} = HC \cdot RA \cdot \left(\frac{T_{max} + T_{min}}{2} + HT \right) \cdot (T_{max} - T_{min})^{HE} \tag{3.5}$$

where RA is in the same unit of ET_P and it is the extraterrestrial radiation, HE in an empirical exponent and it is equal to 0.5, and T_{min}, T_{max} are respectively the daily minimum and maximum temperature expressed in Celsius [33].

The effective evapo-transpiration (ET) is the sum of the effective evaporation and the effective transpiration:

$$ET = E + T \tag{3.6}$$

Both terms can be evaluated as a fraction of the potential evapo-transpiration depending on the water content at time t and on the percentage of soil covered by vegetation (f_v) or percentage of bare soil (*1-*f_v):

$$\begin{aligned} E &= \alpha(\theta_t) ET_p (1 - f_v) \\ T &= \beta(\theta_t) ET_p f_v \end{aligned} \tag{3.7}$$

where α and β are coefficients depending on humidity:

$$\begin{aligned} \alpha &= 0.082\ \theta_t + 9.173\ \theta_t^2 - 9.815\ \theta_t^3 \\ \beta &= \frac{\theta_t - \theta_{wp}}{\theta_{lim} - \theta_{wp}} \end{aligned} \tag{3.8}$$

where θ_{lim} and θ_{wp} are parameters that define the state at which soil moisture becomes limiting and eventually causes vegetation to wilt and transpiration to cease, respectively [34] [25].

Diffusion wave

The superficial runoff routing, throughout the hillslope and the river network, is performed via a diffusion wave scheme, based on Munskingum-Cunge method in its non-linear form with the time-variable celerity. The model computes the surface runoff in each cell and propagates it along any reach of the basin flow path. The method uses both temporal and spatial discretization. The space is subdivided into a section which length is Δs, that is equal to the distance, along the line of maximum slope, between two cells of the grid of the basin; the time subdivision is set during the configuration of the model. In figure 3.4 is reported a scheme of the discretization, Q_i is the inflow discharge in a single cell and Q_{i+1} is the outflow discharge.

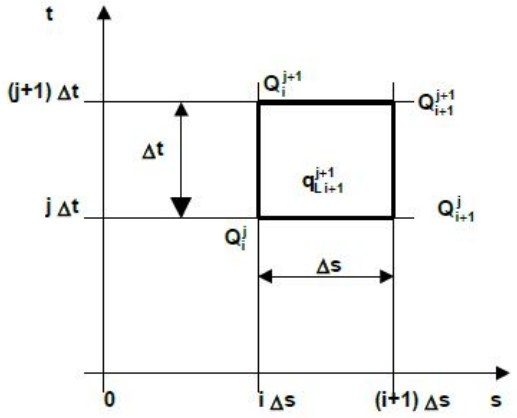

Figure 3.4: Discretization scheme of the Muskingum-Cunge method

The routing scheme is given by:

$$Q_{i+1}^{j+1} = C_1 Q_i^{j+1} + C_2 Q_i^j + C_3 Q_{i+1}^j + q_{i+1}^{j+1} \tag{3.9}$$

where q_{i+1}^{j+1} is the lateral inflow rate to a cell of type channel; $C_r, \ \ (r = 1, \ 2, 3)$ are the routing coefficients and are obtained by using the continuity equation for the channel between the i and $i+1$ nodes, and with the assumption that the storage volume W is a linear function of inflow and outflow discharge. Routing coefficients

are expressed as:

$$\begin{aligned} C_1 &= \frac{\Delta t - 2\tau\varepsilon}{2\tau(1-\varepsilon) + \Delta t} \\ C_2 &= \frac{\Delta t + 2\tau\varepsilon}{2\tau(1-\varepsilon) + \Delta t} \\ C_3 &= \frac{2\tau(1-\varepsilon) - \Delta t}{2\tau(1-\varepsilon) + \Delta t} \end{aligned} \tag{3.10}$$

where τ is a coefficient related to the mean time taken by the wave to propagate along the channel and ε is a dimensionless weighting factor. The lateral inflow rate of the equation (3.9) is expressed as:

$$q_{i+1}^{j+1} = A_0 \frac{P_{e_{i-1}}^{j+1}}{\Delta t} \tag{3.11}$$

with $P_{e_{i-1}}^{j+1}$ denoting direct runoff rate from the elemental cell *i+1* with area A_0 as integrated in time from $j\Delta t$ to $(j+1)\Delta t$. [35]

3.3 Adjustment of the model

A hydrological simulation system needs to be setting for the study area. This procedure is divided into two parts: calibration and validation. Actually, there is a third part that is the initialization, the model needs this phase to determine some parameters and initial conditions for the simulation. The inputs data of temperature and precipitation are measured per minutes from 1st January 2013 to 31th December 2020. The first year is used for the initialization, then the calibration is done from 2013 to 2017 and the validation from 2017 to 2020. These processes consist in a comparison between the simulated superficial discharge with the FEST-WB model and the one calculated with the measured data.

The discharge is calculated in all the stations in which the measure of water depth and water velocity were available (figure 2.11 on page 20). In some sections the obtained discharge was too high for the sections and the type of basin, this probably is due to an error in the measures of water velocity. For this reason, for the model adjustment, is safer to choose a section in which the discharge is more realistic: the section examined is the 106 called *3 Aguas*. Despite of this, it's probably that also in section 106 there are some uncertainty in values of flow rate.

The examined station is located at the beginning of the basin (figure 3.5), just downstream of a confluence of three tributaries. In figure 3.6a is reported the Medellín elevation profile from the source to the station under consideration and in figure 3.6b can be seen a scheme of the soil cover of the sub-basin. Some

characteristics of the sub-basin drained by section *3 Aguas* are reported in table 3.1.

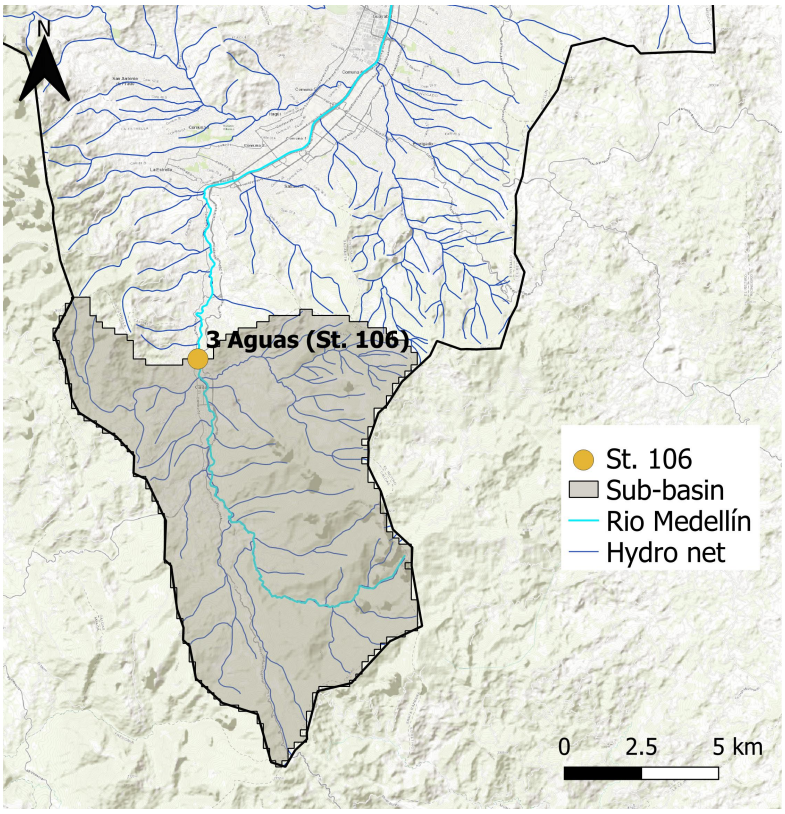

Figure 3.5: Position of station 3 Aguas

Sub-basin 3 Aguas	
Area [km²]	98.16
Main channel [km]	13.73
Basin mean slope [%]	38.79
Main channel mean slope [%]	3.94

Table 3.1: Morphological characteristics of the sub-basin of section 3 Aguas

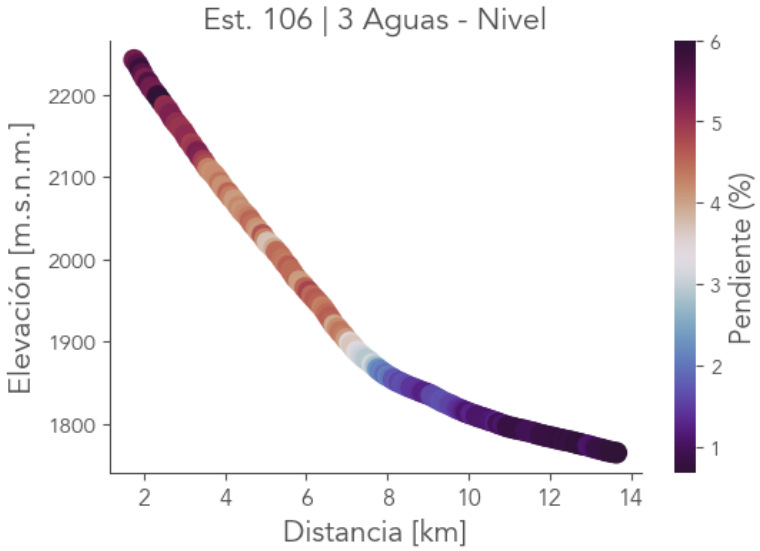

(a) Elevation profile

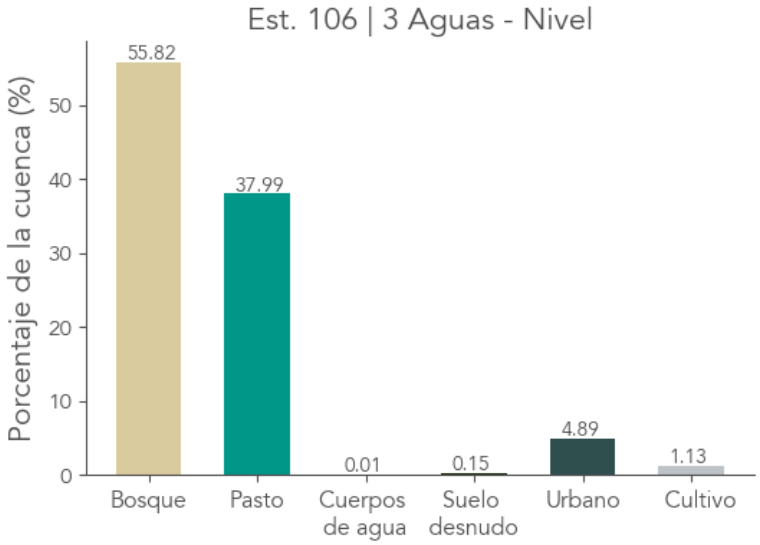

(b) Soil cover

Figure 3.6: Morphology of the sub-basin of section 3 Aguas

Flow rate calculation

Values of discharge in section *3 Aguas* are not directly available but need to be calculated through the data of velocity and water depth. This second variable is available from January 2014 to December 2020, but the velocity, in section 106, is measured only from June 2016[2]. For this reason, the discharge Q is calculated with two different methods. It is computed with a time interval equal to 15 minutes because lower time intervals can cause instabilities in the FEST-WB model, generally it is used a bigger time interval but the nature of the event in this area suggests the use of small intervals.

Knowing the survey of section *3 Aguas* (figure 3.7) it's possible to extract the equation that relates water depth and wet area. Through software HEC-RAS it's possible to obtain the value of wet area when water depth change, therefore it's possible to acquire pairs of points of water depth h and corresponding wet area A. The following equation is obtained interpolating these points:

$$A(h) = -0.7886h^3 + 4.8508h^2 + 6.1023h \tag{3.12}$$

For the period between June 2016 and the end of 2020, a value of the wet area for each measure of water depth can be obtained, then, it's possible to calculate the flow rate with the continuity equation:

$$Q = VA \tag{3.13}$$

During this process there is the assumption that the measured velocity is the mean one. Once, it's known the discharge with the variation of the water depth, it's possible to reconstruct the rating curve for section *3 Aguas* (figure 3.8). The interpolating equation of flow rate and water depth values is a power law with the following coefficients:

$$Q = ah^b = 17.12h^{1.64} \tag{3.14}$$

The equation (3.14) is used to find values of flow rate for the period in which there are only measures of water depth.

The flow rate in Medellín river in correspondence of station *3 Aguas* is reported in figure 3.9. Values calculated with the continuity equation are symbolized in black while values computed with the rating curve are in blue. Observing figure 3.9 it's clear that there is a significant difference between the two methods. It's reasonable to say that discharges computed with power-law are subject to greater approximations. That is because of the precision of the interpolation curve, in fact the series of points in figure 3.8 is difficult to interpolating since it is scattered.

[2]Figure 3.7 reports a previous installation date but during the first months of activity there are only *no data*

Negative values in figure 3.9 correspond to the no value of velocity or water depth present in the data, and also the registered values of water depth that overcome the maximum height of the river banks are equal to no data. In figure 3.9 is also reported, hour by hour, the measure of mean precipitation calculated by the hydrological model in the sub-basin.

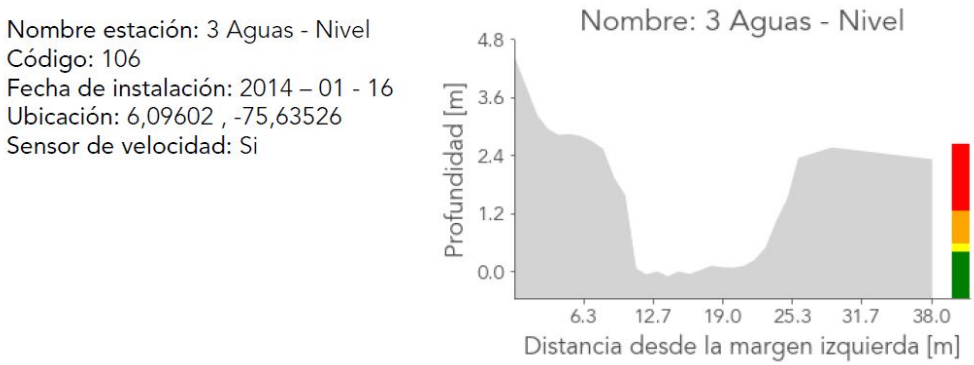

Figure 3.7: Geometry of the section 3 Aguas

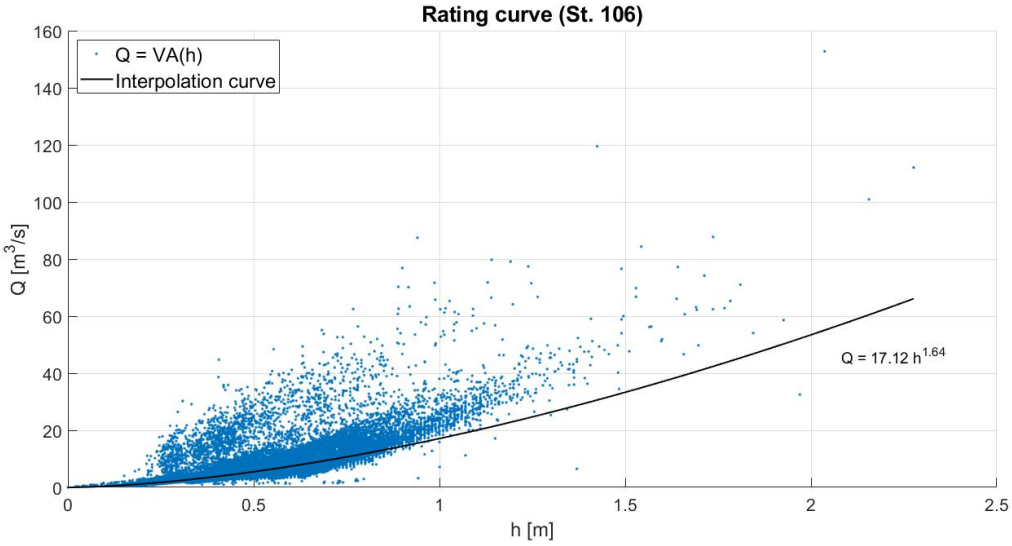

Figure 3.8: Rating curve for the section 3 Aguas

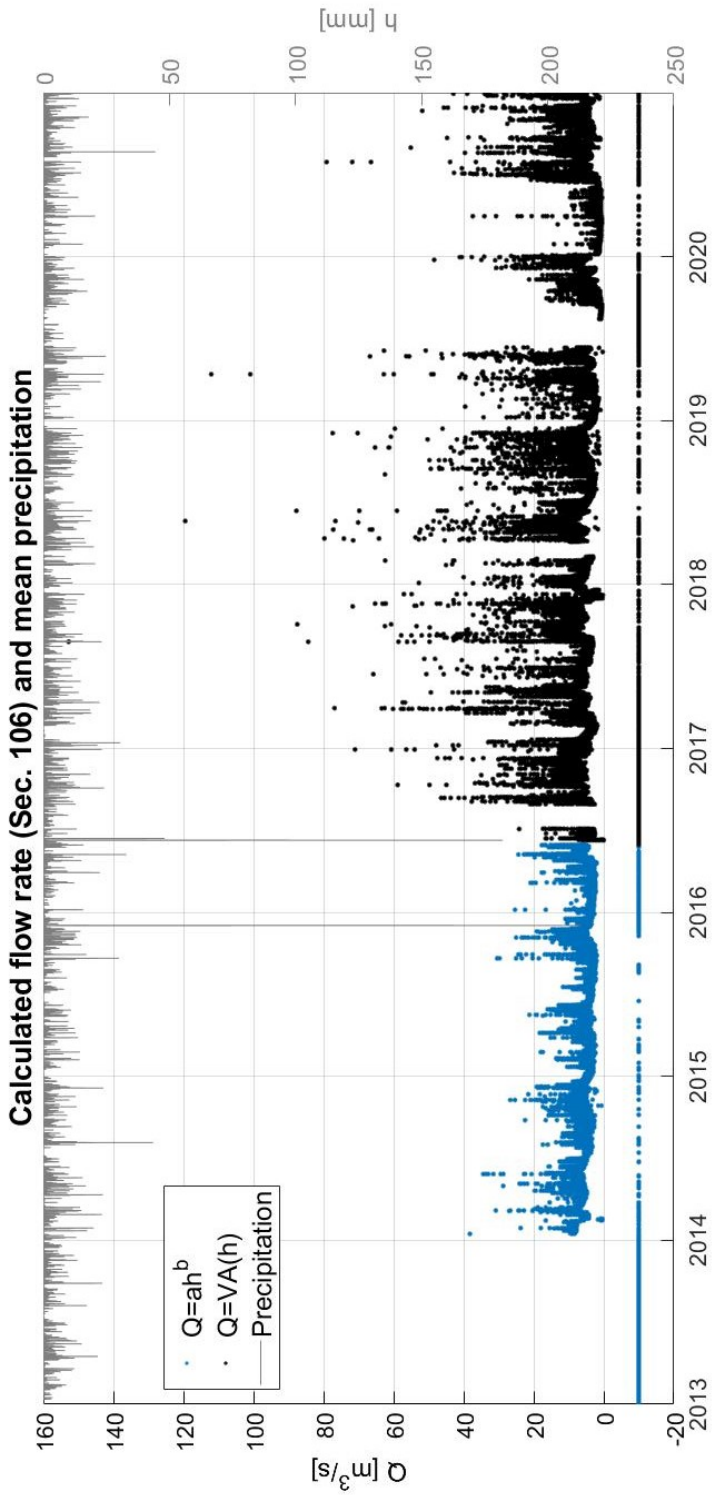

Figure 3.9: Flow rate calculated in section 3 Aguas and mean precipitation in its sub-basin

Calibration

The phase of calibration includes the modification of some parameters in the FEST-WB model in such a way that the simulated hydrograph becomes equal as possible to the calculated hydrograph. The calibration activity is based on the "trial and error" approach, this procedure consists of changing parameters until satisfying results are obtained [21]. In this way there is not unique solution because it's possible to have more than one combination of parameters that optimize the solution.

The comparison between calculated values of discharge and the simulated ones is performed through some indexes that suggest the quality of the adaptation of the two data sets. Three indexes investigated are:

- Root Mean Square Error [m^3/s]:

$$RMSE = \sqrt{\frac{1}{n}\sum_{i=1}^{n}\left(Q_{obs}^{i} - Q_{sim}^{i}\right)^2} \tag{3.15}$$

  where the subscript *obs* indicates the discharge calculated through observed variable. The root mean square error can be between 0 and $+\infty$, a value equal to 0 means that the simulated flow rate corresponds to the calculated one.

- Nash-Sutcliffe index:

$$E = 1 - \frac{\sum_{i=1}^{n}\left(Q_{obs}^{i} - Q_{sim}^{i}\right)^2}{\sum_{i=1}^{n}\left(Q_{obs}^{i} - \overline{Qobs}\right)^2} \tag{3.16}$$

  this second index considers the quality of the simulation in respect to the mean of calculated values; it assumes values between $-\infty$ and 1, if it is equal to 1 it means that there is a perfect representation of the phenomenon, if it is less than 0 than the mean of the calculated values is better than the simulated ones

- Mean bias:

$$\bar{\varepsilon} = \frac{1}{n}\sum_{i=1}^{n}\left(Q_{sim}^{i} - Q_{obs}^{i}\right) \tag{3.17}$$

  it is the mean of the error of each value of Q, it is useful to understand if there is a underestimation ($\bar{\varepsilon} < 0$) or an overestimation ($\bar{\varepsilon} > 0$)

In addition to indexes, a graphic method is used in which the shape of the curves of accumulated volumes is compared.

The choice of the best combination of parameters is a compromise between a perfect reproduction of the cumulated volume curve and ideal values for the indexes.

In view of choosing which parameters are more logical to modify and how to modify it, it's useful to do a first simulation (*sim 0*). That is important to understand how the hydrological model reacts to the input and, consequently, what's necessary to modify.

Parameters modified during consecutive calibrations are, initially, two:

- saturated conductivity k_{sat} [m/s] that is the vertical permeability that controls the infiltration and, therefore, the superficial flow rate; initially it is equal to the mean value for the type of soil present in the basin (clay loam): $k_{sat} = 6.39 \cdot 10^{-7}\ m/s$

- subsurface permeability $k_{sat,sub}$ [m/s], that is the horizontal permeability in active layer of soil and it influences the velocity of the subsurface flow so the base flow in the river; in the first simulation it is equal to the saturated conductivity, then it is possible to change it through a scale factor.

After some simulations, another parameter has been modified due to the two parameters contributions were not satisfying. The third parameters was the depth (Z) of the soil considering in the water balance. An increase of this value has as a consequence an increase of the infiltration. Initially, the depth of the active soil is equal to 1 meter.

In table 3.2 are reported the values of the parameters and the adaptation indexes for each simulation. The best values of the parameters are highlighted in green however, the best simulation is the number 14 (highlighted in yellow) because it reproduces accurately the curve of the cumulated volume. The cumulated volume curves from 2014 to 2017 are reported in figure 3.10, the calculated curve is in black, in red there is the one of the chosen simulation (*sim 14*) and the green curve represents the cumulated volume for the first simulation (*sim 0*).

In figure 3.11 are reported the flow rate in section 3 Aguas (st. 106) for the time period of calibration, it is clear that the simulation 0 didn't reproduce the base flow in the river and it presents numerous high peaks. The base flow is given by the infiltrated water that constantly reaches the river. If there is a low base flow for a long time simulation it means that there is a low rate of infiltration and the infiltration flow reaches almost immediately the river. To intensify this contribution, saturated conductivity and subsurface permeability was increased.

Also the raise of depth gives a contribution because it increases the time with which waters reach the river.

The simulations generated some very high peaks, probably because of some instability of the model, to overcame this problem, for the simulated discharge has been fixed a maximum level that corresponds to the maximum value of discharge observed. The negative values in figure 3.11 are the ones that overcome the maximum discharge.

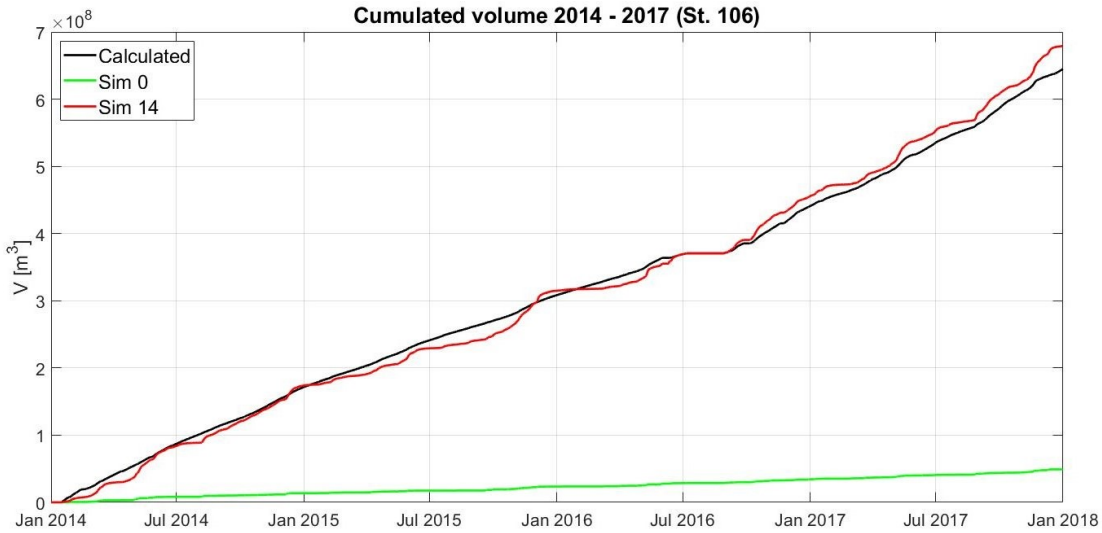

Figure 3.10: Cumulated volume for the period of calibration

Sim. n°	k_{sat} [m/s]	$k_{sat,sub}$ [m/s]	Z [m]	RMSE [m^3/s]	E [-]	$\bar{\varepsilon}$ [m^3/s]
0	6.39E-07	6.39E-07	1	7.18	-3.43	-5.32
1	6.39E-07	6.39E-04	1	6.65	-3.43	-5.32
2	6.39E-07	6.39E-02	1	6.32	-3.00	-4.96
3	6.39E-05	6.39	1	5.95	-2.45	-5.13
4	6.39E-06	0.64	1	6.07	-2.59	-5.20
5	6.39E-05	31.94	1	5.80	-2.27	-2.04
6	6.39E-06	3.19	1	5.62	-2.08	-2.50
7	6.39E-05	31.94	1	5.68	-2.14	-2.06
8	6.39E-05	63.89	1	9.89	-8.90	1.61
9	6.39E-05	44.72	1	7.16	-4.03	-0.53
10	6.39E-04	447.22	1	8.31	-5.93	0.25
11	6.39E-06	4.47	1	6.62	-3.27	-1.18
12	6.39E-04	447.22	0.5	10.54	-11.15	0.20
13	6.39E-04	447.22	2	6.30	-2.87	0.30
14	6.39E-04	447.22	2.5	5.91	-2.40	0.31
15	6.39E-05	44.72	2.5	5.32	-1.75	-0.60
16	6.39E-05	51.11	2.5	5.84	-2.32	0.14
17	6.39E-04	511.11	2.5	6.66	-3.33	1.18
18	6.39E-04	511.11	2	7.27	-4.15	1.17

Table 3.2: Procedure of calibration: calibration parameters and adaptation indexes

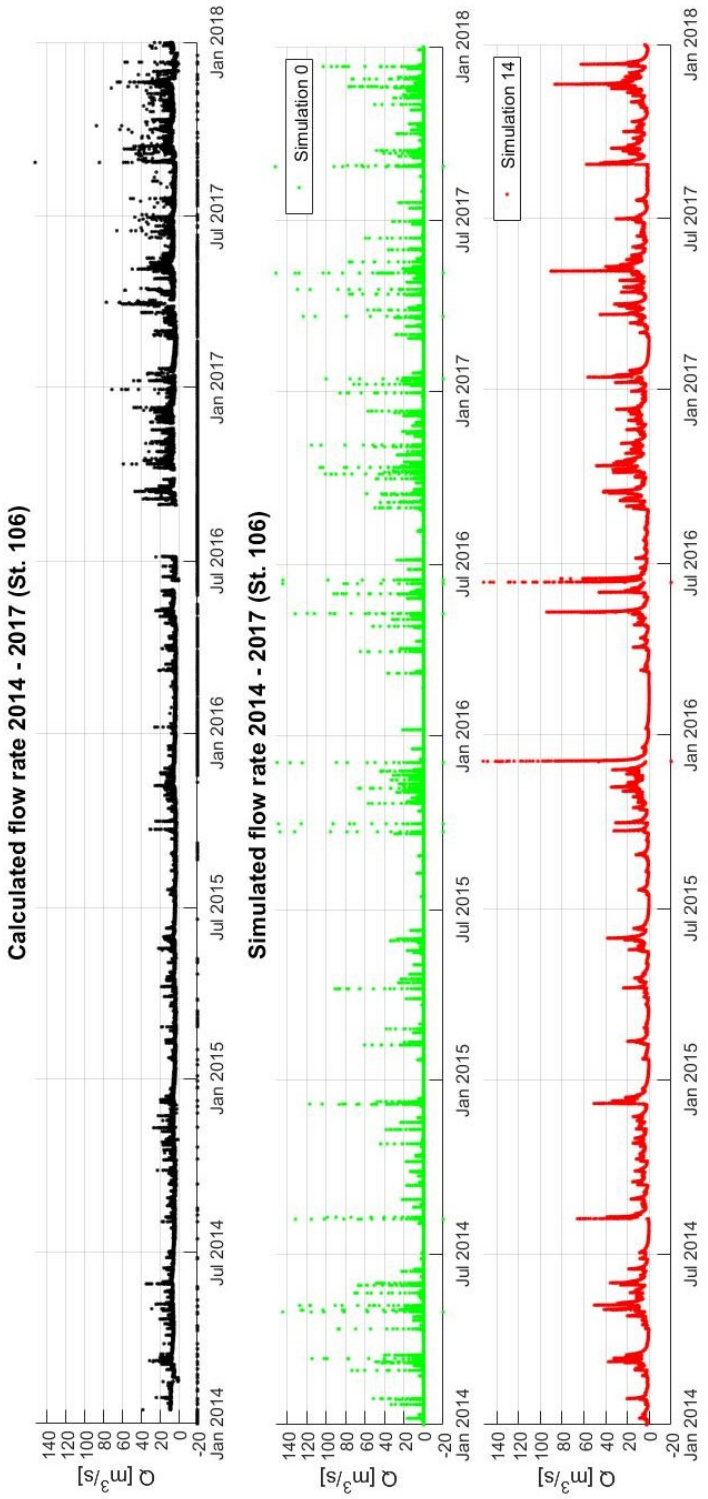

Figure 3.11: Simulated discharge for the period of calibration

	RMSE [m³/s]	**E [-]**	$\bar{\varepsilon}$ **[m3/s]**
Calibration (2014-2017)	5.91	-2.40	0.31
Validation (2018-2020)	6.89	-1.61	2.44

Table 3.3: Indexes for validation and calibration

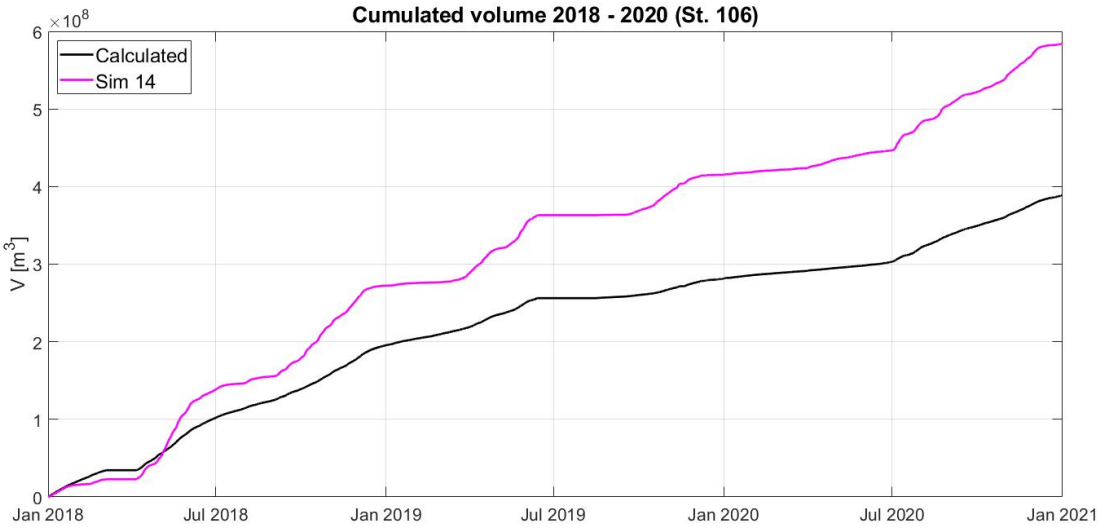

Figure 3.12: Cumulated volume for the period of validation

Validation

The validation consists of comparing the calculated discharge with the simulated one for a time period different from the one of calibration. This phase is useful to understand if the result of the model can be satisfying also for a data set in which the model isn't calibrated.

In figure 3.13 are reported the calculated discharge and the simulated flow rate with simulation number 14 from 2018 to 2020. To understand if the model is acceptable also for this period it's necessary to calculate adaptation indexes (table 3.3) and cumulated volumes (figure 3.12). Values of the indexes are worst respect to the ones calculated for the calibration, also the curve of cumulated volumes is not so similar to the observed one. There is a stronger overestimation in respect to the calibration period. Looking at the graph (figure 3.14) with cumulated volumes for the entire period, from 2013 to 2020, it is clear that the overestimation starts from the half of 2016. June 2016 is the date in which there is a change between the method through which the flow rate is calculated. In fact, from June 2016 there is an increase of discharge and so an increase of cumulated volume. This underline the importance to have measured discharge data to do an efficient calibration

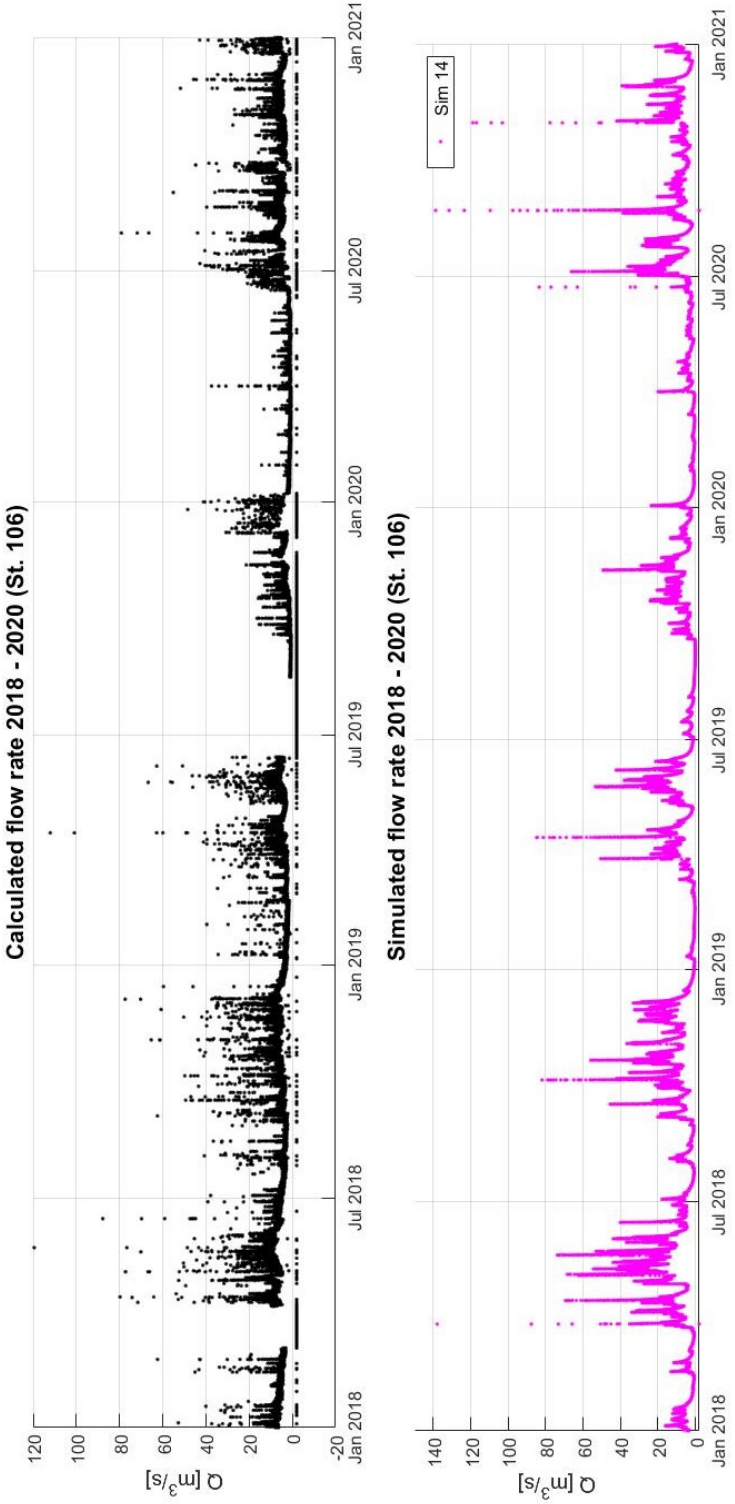

Figure 3.13: Simulated discharge for the period of validation

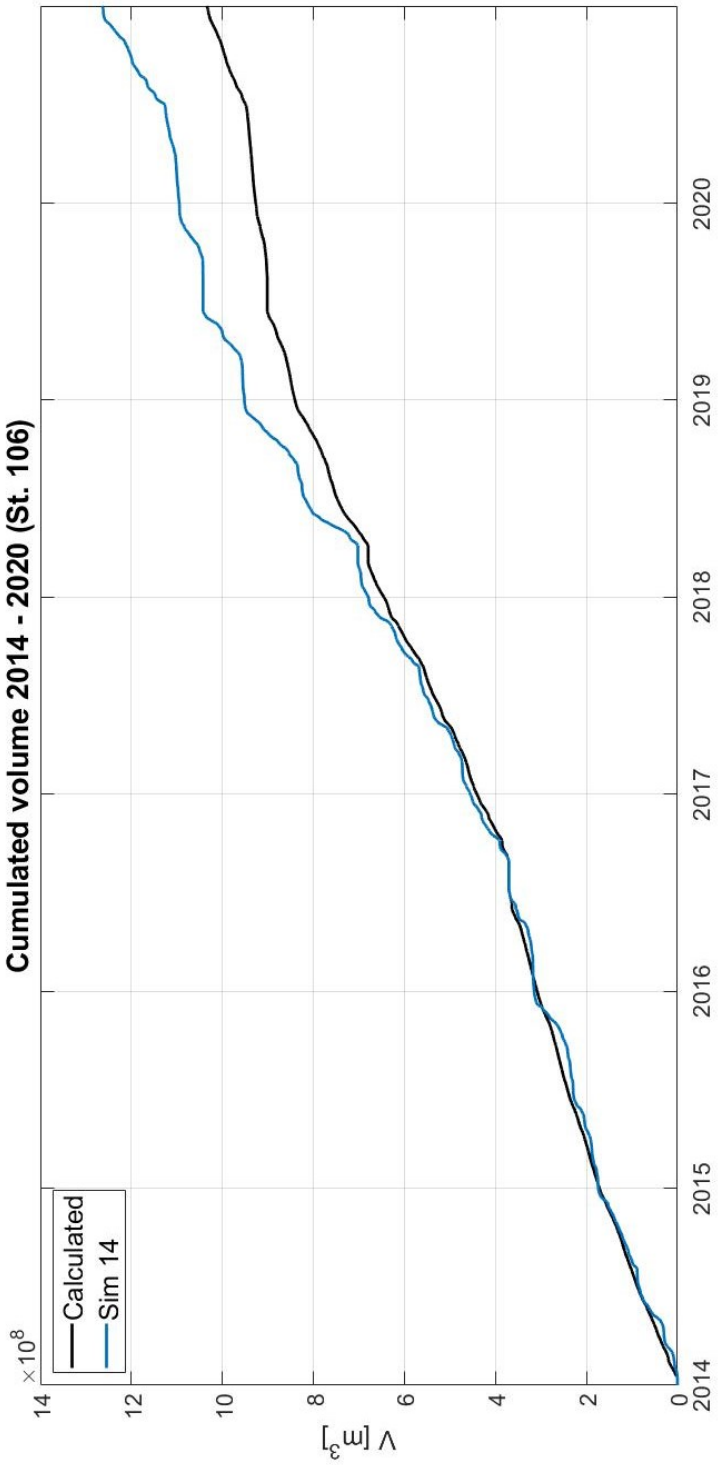

Figure 3.14: Cumulated volume for the entire period of study

Chapter 4

Application with forecast inputs

The last phase of this study consists of applying the hydrological model starting from the forecast date of temperature and precipitation. This is important because the ultimate aim is to use the hydrological model as a warning system, so the purpose is to be able to alert the responsible bodies when forecast data are available and not only some hours before of an event when measured data are available.

For this procedure two important events of 2020 have been chosen. The first analysed period is from 31 August 2020 to 05 August 2020 (*Event 1*), the second is from 27 November 2020 to 2 December 2020 (*Event 2*) [36] [37]. In both periods there are heavy rainfalls with peaks of discharge, and consequently floods of Medellín river. The analysis is done not only on section *3 Aguas* (sec. 106), the one on which the model was calibrate, but also for the sections *Aula Ambiental* (sec. 99), *Puente Fundadores Copacabana* (sec. 140) and the closing section of the basin *Puente Gabino* (sec. 260); in figure 2.11 on page 20 is reported the position of these sections, they are all in the main channel of the basin.

4.1 Meteorological model

The meteorological model used is the Global Forecast System, a weather forecast model produced by the National Centers for Environmental Prediction (*GFS, NOAA/NCEP, USA*) [38] [39]. It is a global open access model, as it covers the entire globe. The GFS model is a coupled model, composed of four separate models (an atmosphere model, an ocean model, a land/soil model, and a sea ice model), which work together to provide an accurate picture of weather conditions. The model has a horizontal resolution of 0.5 that, at the equator, corresponds to 50 km, the time resolution is three hours. Values of variables are available at different altitudes, in this study the layer of interest is the lower one so the precipitations are forecast at the altitude of the ground and temperature two meters above.

Output of the meteorological model

Outputs of the meteorological model consist of a grid with cells which dimensions are 50 km x 50 km. The basin is covered by only three cells (figure 4.1), so there are only three values of precipitation every three hours for the entire basin. It's clear that the resolution of this forecast is not appropriate for the basin; a more accurate study can be done thorough a local system of meteorological forecast.

In figure 4.2 are reported the mean cumulated precipitation interpolated in the sub-basins identified by the sections. Continuous lines represent the precipitation calculated from the measured data while dashed lines are the forecast precipitation. For the event 1 (figure 4.2a) there is an over-estimation of the precipitation by the meteorological model during all the period; the event seems to be more intense in the downstream sections (sections 140 and 160) in comparison to the upstream ones. In the second period, there is initially an underestimation of the rainfall due to a localized event, and higher precipitation is registered and forecast in the upstream sections (section 106 and 99). From the maps of precipitations reported in appendix A, it's possible to deduce the same results and to better understand the spatial distribution. These maps are available in terms of daily cumulated rainfall.

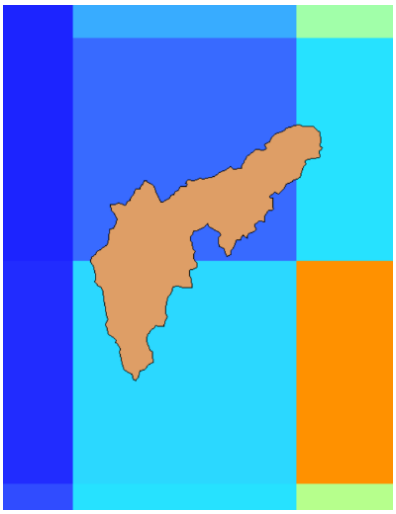

Figure 4.1: Resolution of the meteorological model in respect to the basin

4.2 Analysis of the hydrographs

The way to understand the quality of the hydrological simulation with forecast precipitation is to see if it is able to simulate an observed flood. The focus is on

		Observed event: Yes	Observed event: No
Forecast event	Yes	Correct positive	False alarm
	No	Missed alarm	Correct negative

Table 4.1: Contingency table

the overcome of the threshold discharge that causes the flood. In the contingency table (4.1) are resumed the four possible scenarios. The worst scenario is the *missed alarm*, in this case, the flood will not be forecast but it will happen. The case of *false alarm* it's not dangerous but if there are a lot of false alarm consequently the model will no longer be deemed reliable. Of course, this type of analysis is more accurate when is analysed a significant number of events or periods. In this study only two period are analysed, however it can be significant for future studies.

For each measuring section warning threshold are fixed by SIATA. Four different levels are identified:

- N1 - Safe water level: it isn't registered change in water depth that can bring to a flood
- N2 - Attention level: there is a raise in water depth, it is the previous phase of a possible flood
- N3 - Flood of minor importance: flood affects street and building near the river
- N4 - Important flood: flood extended to building and street, it is necessary to evacuate the population in the affected area

The chosen level for the threshold is the N3 for all section. In figure 4.3 are reported the surveys of sections of interest and the registration of the water depth[1] with the warning threshold. For all the sections was calculated the discharge as is describe in section 3.3 for the station *3 Aguas*. Appendix B reports the rating curves. So, for each section, it's possible to calculate the discharge for the warning level through the power-law of the section. In table 4.2 are written the warning water level and discharge for all the examined sections.

The figures 4.4, 4.5, 4.6 and 4.7 show the hydrographs of the two selected period for each sections. There is also reported the hyetograph of forecast precipitation with a time step of three hours that is the time resolutions of the meteorological model. The flow rate calculated from the observed data is reported with black dots

[1]These registrations of water level are taken in the morning of the 30 June 2020

	Section	h_{N3} [m]	$Q_{threshold}$ [m^3/s]
99	Aula Ambiental	1.9	68.5
106	3 Aguas	0.9	14.4
140	Puente Fundadores Copacabana	3.1	88.76
260	Puente Gabino	7	334.85

Table 4.2: Water depth and discharge threshold

while the blue curve are the simulated discharge, the dashed one stand for the flow rate simulated with forecast input. In each graph, the simulation with forecast data overestimate the discharge both for the base flux and the peaks. This can cause false alarms but on the other hand this simulation it's more accurate, during the flood, with respect to the simulation with observing data. It's possible to say that the overestimation of the simulation with forecast provides the underestimation of the simulation with measures.

In the hydrographs is also reported the threshold discharge. In all sections, for both periods, both the calculated discharge and the one simulated with forecast overcome the threshold. Referring to table 4.1 on the preceding page all sections, for both events, are in the scenario of correct positive.

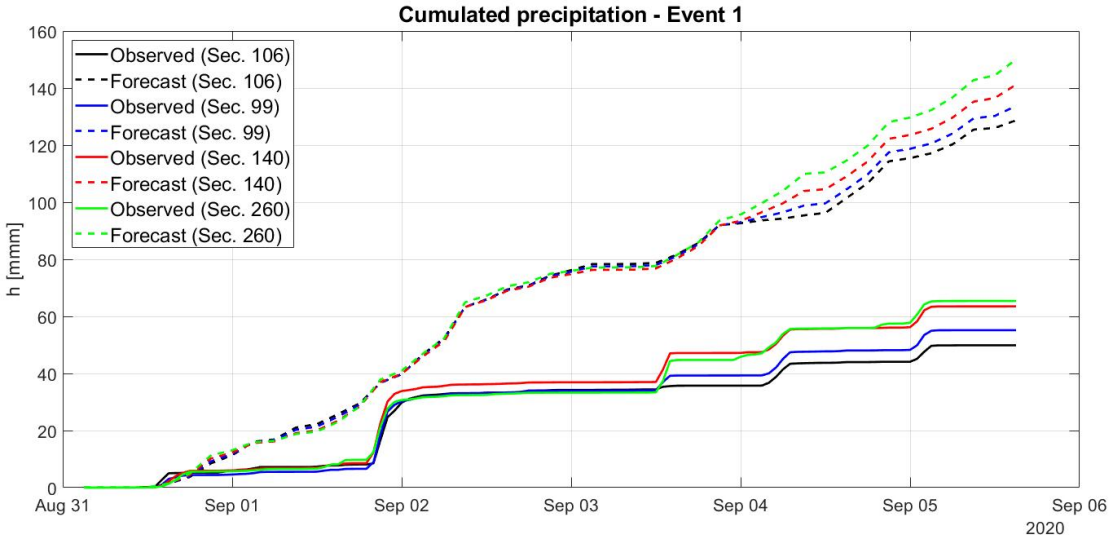

(a) First period

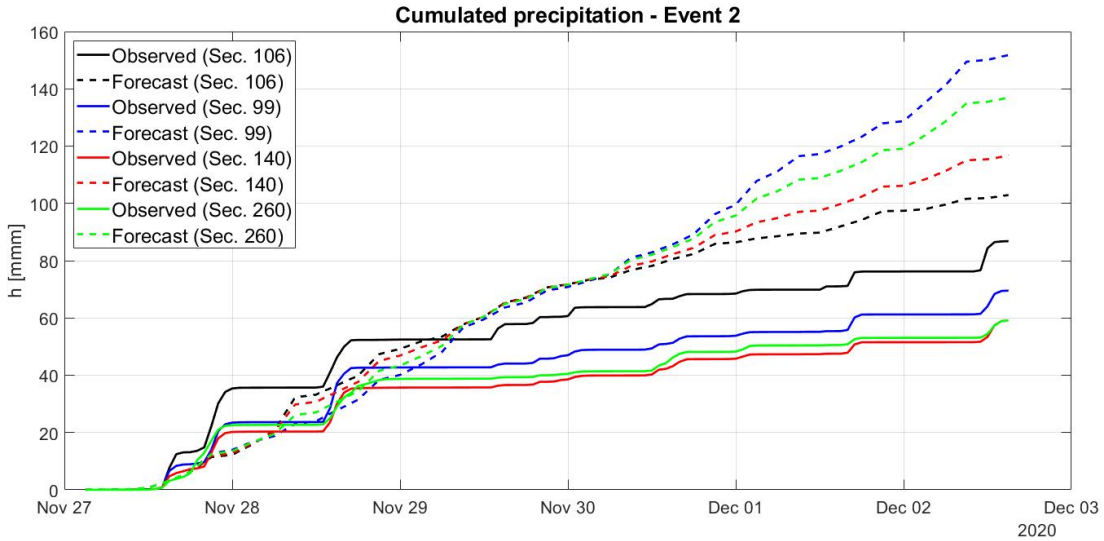

(b) Second period

Figure 4.2: Observed and forecast cumulated precipitation

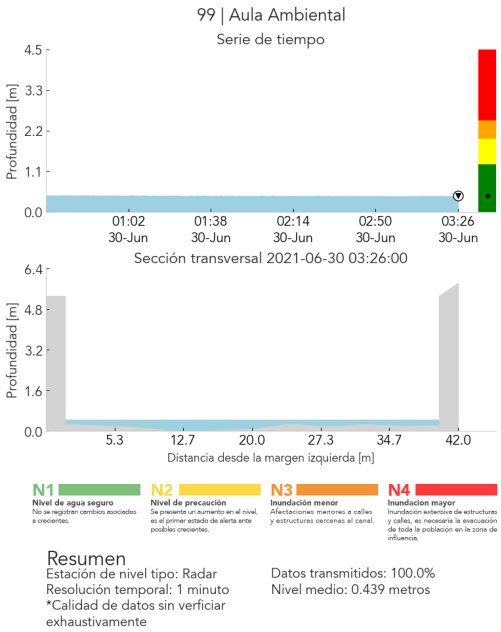

(a) Section 99 Aula Ambiental

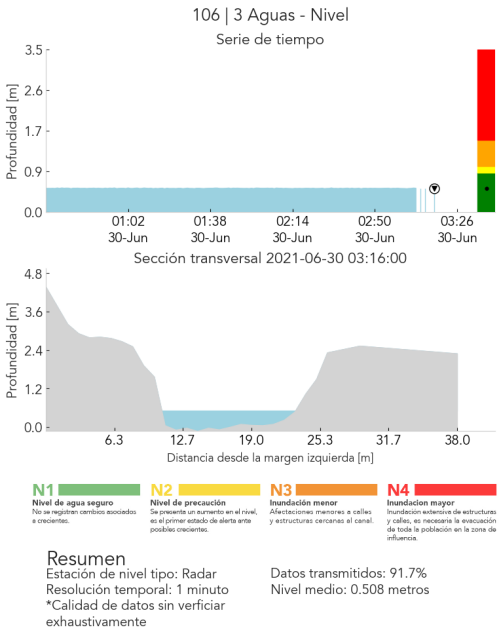

(b) Section 106 3 Aguas

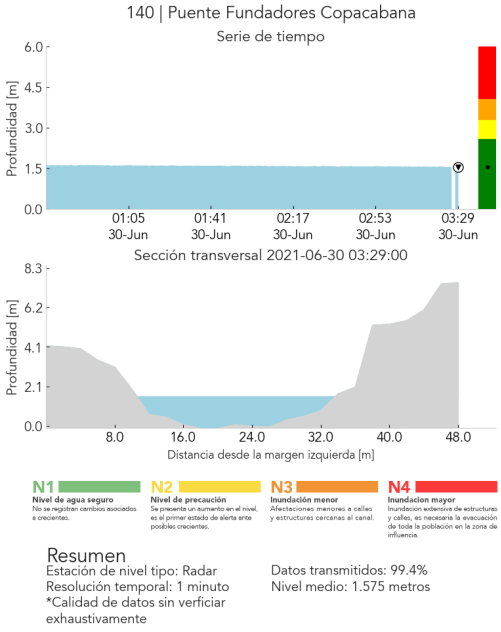

(c) Section 140 Puente Fundadores Copacabana

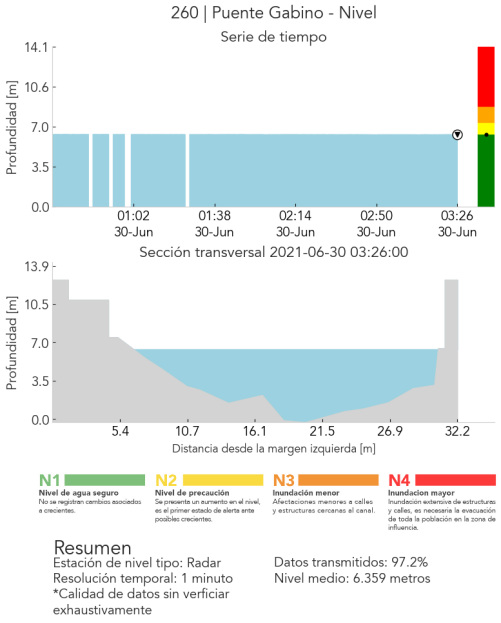

(d) Section 260 Puente Gabino

Figure 4.3: Surveys and warning level for the examined sections [1]

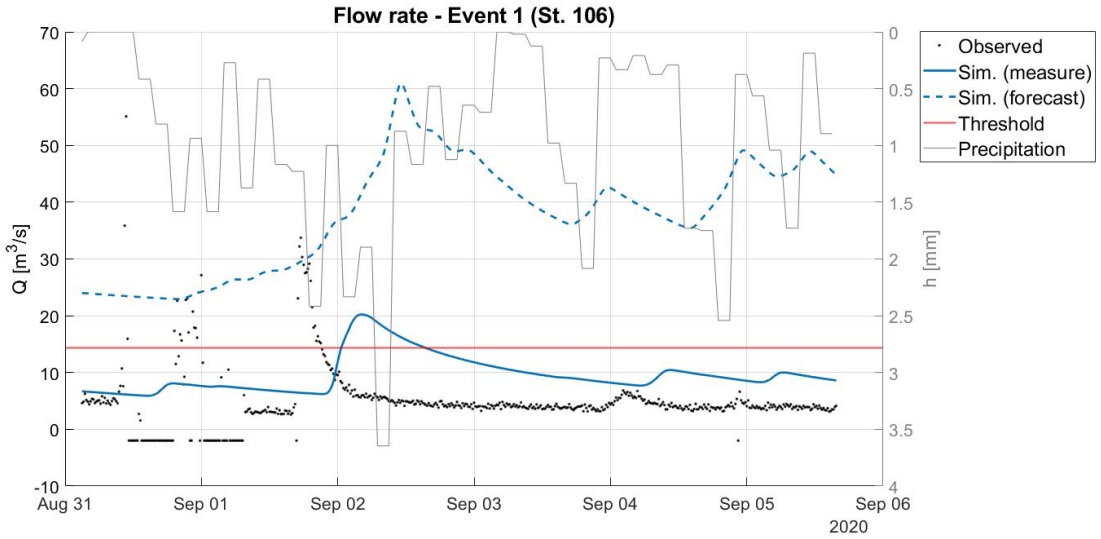

Figure 4.4: Hydrographs for section 106 in the first period

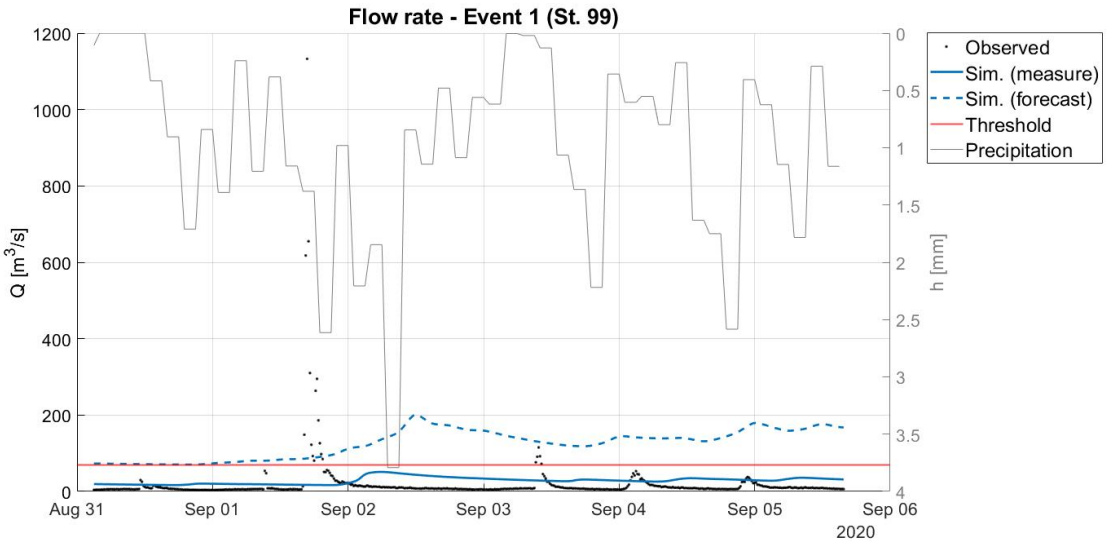

Figure 4.5: Hydrographs for section 99 in the first period

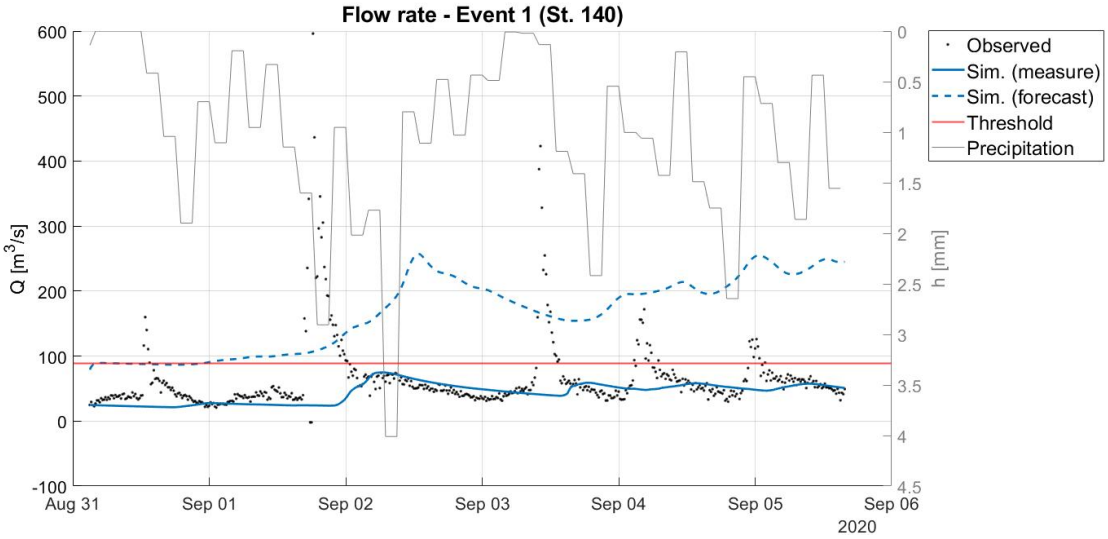

Figure 4.6: Hydrographs for section 140 in the first period

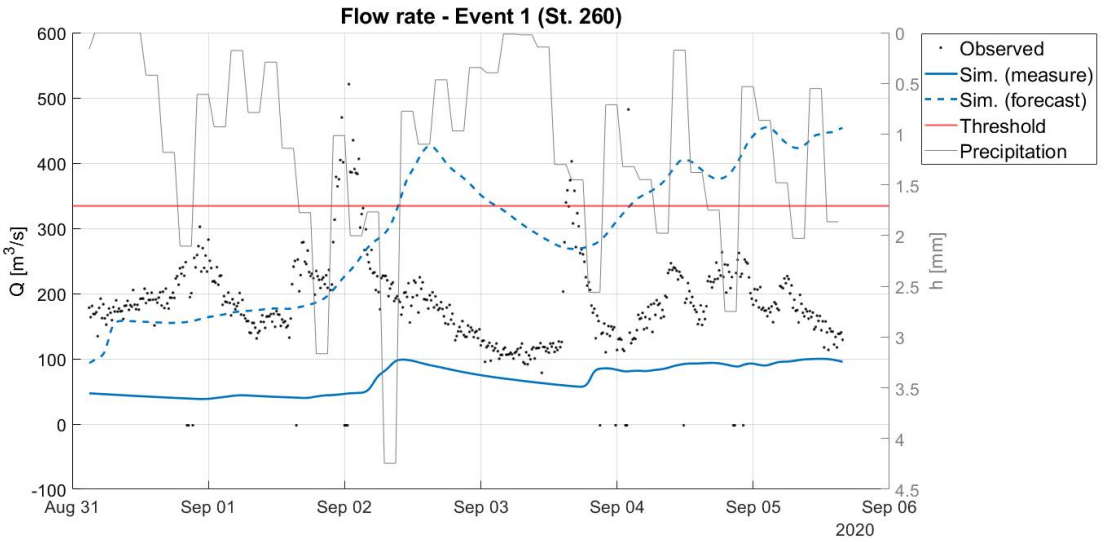

Figure 4.7: Hydrographs for section 260 in the first period

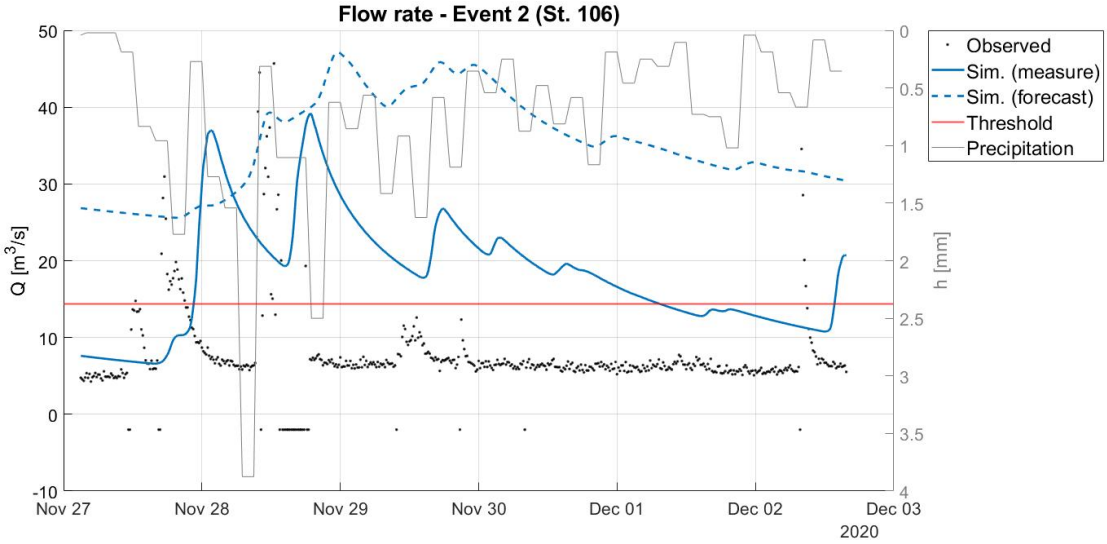

Figure 4.8: Hydrographs for section 106 in the second period

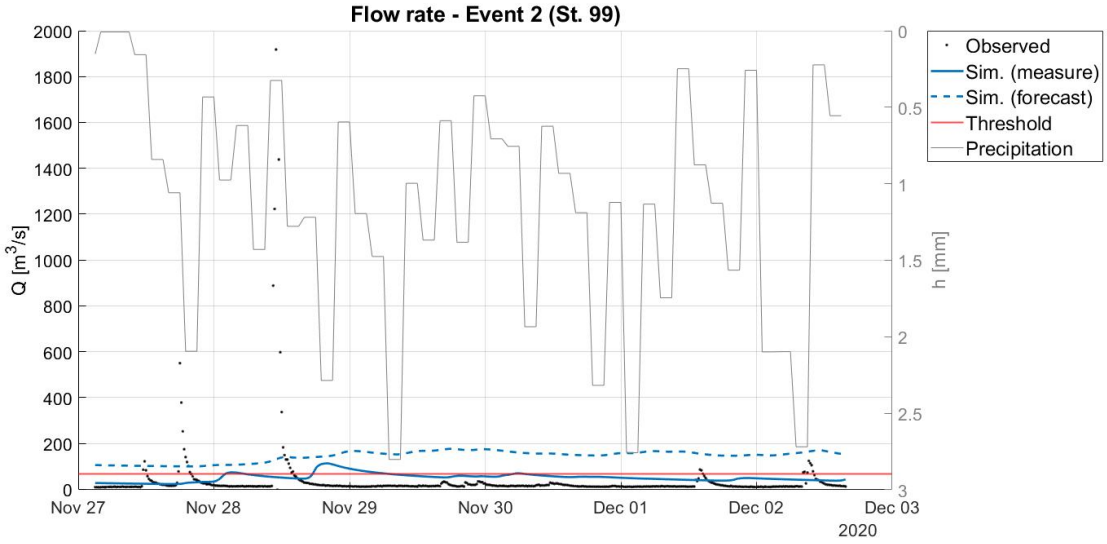

Figure 4.9: Hydrographs for section 99 in the second period

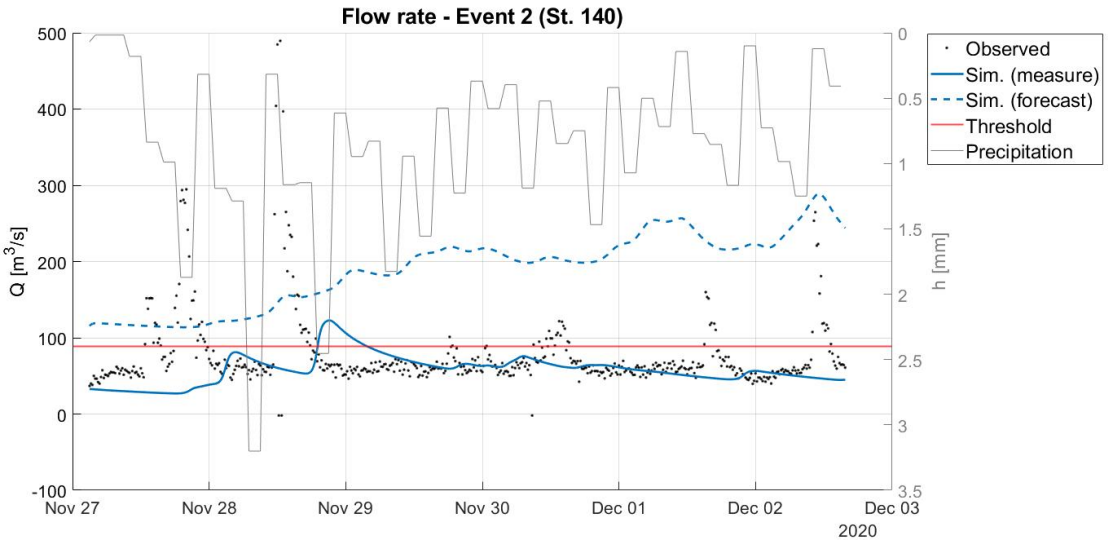

Figure 4.10: Hydrographs for section 140 in the second period

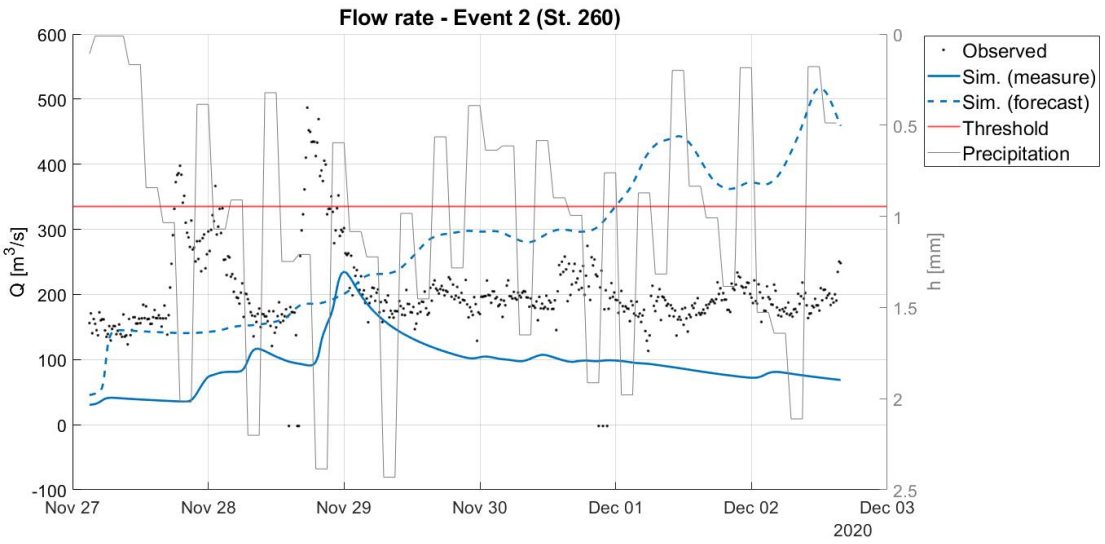

Figure 4.11: Hydrographs for section 260 in the second period

Chapter 5

Conclusion

In the present thesis the hydrological FEST model has been applied to the Medellín river basin for evaluating its capacity of flood forecasting. The calibration and validation have been carried out through an important network of measurement stations located in the whole basin and developed by SIATA. Subsequently, two precipitation events were analysed using forecast data as input, and then compared to measured data. This procedure allowed to understand if the hydrological model can be used as a warning system.

The adjustment of the FEST-WB model showed that it is possible to apply it to this type of basin with such meteorological conditions. In the two analysed events, the model used with forecast input shows *correct positive* in the warning analysis. This means that, in these cases, the documented flood would have been forecast by the hydrological model.

The application of the hydrological model underlines the possibility of using it in the watershed of the Medellín river. To do this, it is fundamental to have a solid network of measures in the examined area, which is rarely available. For the model application, a key role has been played by the significant sensor system of SIATA in the area.

Since the available measures referred to the time period from 2013 until the present day, it has been possible to execute a solid adjustment of the model. Nevertheless, it was not possible to adjust the model in the entire basin. This is due to the difficulty in understanding the value of discharge calculated through the measures of water depth and velocity, and also it is due to the scarce information about discharge measurement campaigns or rating curves of the basin. The flow rate in some of the analysed sections seemed to be over-estimated. This was probably due to a mal-interpretation of the water velocity's data. This led to the adjustment of the model in only one small sub-basin. For this reason, during the calibration phase, the attention was on the correspondence of the cumulated

volume curves and not on the adaptation index, because they were calculated on the values of discharge. However, the adaptation indexes after the calibration have reached acceptable values.

Even if the model was calibrated only in an upstream sub-basin the analysis of the two events was done in sections located all along the river Medellín and the results of these phases were satisfying in terms of prediction of floods.

SIATA provided the data used in this work such as: precipitations, temperatures, water depth, water velocity and the surveys of the sections. Recently, they also start to measures other variables, such as wind velocity, air humidity and solar radiation. In the future, when further data will be available, it will be possible to calibrate using more appropriate equations in the FEST-WB model and improving the efficiency of the model.

To ameliorate the application of FEST-WB, it is also possible to calibrate it in more than one sub-basin. For this purpose, it is fundamental to have better information on the flow rate. One possibility is to calculate the discharge without the data of velocity to overcome the issue probably given by this measure. Thanks to the amount of information about the river and its sections, a possible attempt is to calculate the discharge with the Chézy equation.

The last part of this thesis can be expanded with the study of more events and also using input data that comes from a local meteorological model and not a global one.

Bibliography

[1] SIATA. Sistema de alerta temprana de medellín y el valle de aburrá, 4 2021. `https://siata.gov.co/sitio_web/index.php/`.

[2] Juan Pablo Patiño. Diez municipios de antioquia, afectados por las lluvias durante puente festivo, 7 2021. `https://www.elcolombiano.com`.

[3] M. Werner, J. C. Loaiza, M. C. Rosero Mesa, M. Faneca Sànchez, O. De Keizer, and M. C. Sandoval. Developing Flood Forecasting Capabilities in Colombia (South America). *Flood Forecasting: A Global Perspective*, pages 349–368, 2016.

[4] Stephanie Clark, Ashish Sharma, and Scott A. Sisson. Patterns and comparisons of human-induced changes in river flood impacts in cities. *Hydrology and Earth System Sciences*, 22(3):1793–1810, 2018.

[5] P. C.D. Milly, R. T. Wetherald, K. A. Dunne, and T. L. Delworth. Increasing risk of great floods in a changing climate. *Nature*, 415(6871):514–517, 2002.

[6] Sharad Kumar Jain, Pankaj Mani, Sanjay K. Jain, Pavithra Prakash, Vijay P. Singh, Desiree Tullos, Sanjay Kumar, S. P. Agarwal, and A. P. Dimri. A Brief review of flood forecasting techniques and their applications. *International Journal of River Basin Management*, 16(3):329–344, 2018.

[7] L. Alfieri, P. Burek, E. Dutra, B. Krzeminski, D. Muraro, J. Thielen, and F. Pappenberger. GloFAS-global ensemble streamflow forecasting and flood early warning. *Hydrology and Earth System Sciences*, 17(3):1161–1175, 2013.

[8] Luc Feyen, Jasper A. Vrugt, Breanndán Ó Nualláin, Johan van der Knijff, and Ad De Roo. Parameter optimisation and uncertainty assessment for large-scale streamflow simulation with the LISFLOOD model. *Journal of Hydrology*, 332(3-4):276–289, 2007.

[9] J. Thielen, J. Bartholmes, M.H. Ramos, and A. de Roo. The European Flood Alert System – Part 1: Concept and development. *Hydrology and Earth System Sciences Discussions*, 5(1):257–287, 2009.

[10] Efraín Domínguez-Calle and Sergio Lozano-Báez. Estado del arte de los sistemas de alerta temprana en Colombia. *Revista de la Academia Colombiana de Ciencias Exactas, Físicas y Naturales*, 38(148):321, 2014.

[11] Juan-David López-García, Yesid Carvajal-Escobar, and Angélica-María Enciso-Arango. Sistemas de alerta temprana con enfoque participativo: un desafío para la gestión del riesgo en colombia TT - Early warning systems with a participative approach: a challenge for risk management in colombia. *Rev. luna azul*, (44):231–246, 2017.

[12] María Alejandra Ochoa Isaza. *Impacto de la informacíon a partir de radar meterorológico en la simulación hidrológica distribuita: simulación de eventos extremos y ventajas para la gestión del riesgo en la cuenca del río Medellín.* PhD thesis, 2013.

[13] Ministerio de Ambiente y Desarrollo Sostenible (MADS), Corporación Autónoma Regional del Centro de Antioquia (Corantioquia), Área Metropolitana del Valle de Aburrá (AMVA), Corporación Autónoma Regional de las Cuencas de los Ríos Negro y Nare (CORNARE), CPA INGENIERÍA S.A.S, and Fondo Adaptación. Actualización POMCA Río Aburrá. Plan de Ordenación y Manejo de la Cuenca Hidrográfica. page 486, 2019.

[14] GitHub. *Land Cover (GLCNMO) - Global version*, 04 2021. `https://globalmaps.github.io/glcnmo.html`.

[15] ISRIC. *SoilGrids*, 04 2021. `https://soilgrids.org/`.

[16] Rubén A. García-Gaines and Susan Frankenstein. USCS and the USDA Soil Classification System. *UPRM and ERDC Educational and Research Internship Program*, (March):37, 2015.

[17] Oscar Gabriel Cáardenas Hernández. *Segundo lebantamiento integrado de cuencas hidrográficas del municipio de Medellín.*

[18] El colombiano, 5 2021. `https://www.elcolombiano.com`.

[19] Carlos López. Emergencias por aguacero en medellín, sabaneta y envigado, 6 2021. `https://www.elcolombiano.com`.

[20] Ferney Arias Jiménez. Aguacero en medellín causa cortes de energía y suspensión en metrocables, 6 2021. `https://www.elcolombiano.com/antioquia/medellin/balance-lluvias-en-medellin-en-navidad-2020-FF14335154`.

[21] G Ravazzani, D Rabuffetti, C Corbari, and ... Validation of FEST-WB, a continuous water balance distributed model for flood simulation. *31° Convegno Nazionale di Idraulica e Costruzioni Idrauliche*, page 9, 2008.

[22] C Corbari, J Martinelli, G Ravazzani, and M Mancini. Snow satellite images for calibration of snow dynamic in a continuous distributed hydrological model. *Hydrology and Earth System Sciences Discussions*, 4(6):3979–4004, 2007.

[23] G Ravazzani, D Rabuffetti, C Corbari, A Ceppi, and M Mancini. Testing FEST-WB, a continuous distributed model for operationa quantitative discharge forse in the upper Po river. *Analyses and images of hydrological extremes mediterranean enviroment*, pages 115–129, 2008.

[24] Encyclopædia Britannica. Water-cycle, 6 2021. `https://www.britannica.com`.

[25] Elena Angela Maria Corso. *Stime di precipitazione da satellite della costellazione GPM per la modella zione idrologica del bacino del tanaro*. PhD thesis, 2018.

[26] R.H. Brooks and A.T. Corey. Verifica di diversi modelli di infiltrazione nella modellistica a. *Physics and Chemistry of Glasses: European Journal of Glass Science and Technology Part B*, 1964.

[27] Davide Sonvico. *Verifica di diversi modelli di infilitrazione nella modellistica idrologica a scala di bacino in bacini pre alpini e semi-aridi*. PhD thesis, 2017.

[28] Lijun Su, Quanjiu Wang, Yuyang Shan, and Beibei Zhou. Estimating Soil Saturated Hydraulic Conductivity using the Kostiakov and Philip Infiltration Equations. *Soil Science Society of America Journal*, 80(6):1463–1475, 2016.

[29] Voltaggio Simone. Infiltrazione, 5 2021. `https://manualedelgeologo.it/infiltrazione/`.

[30] U Adindu Ruth, K Igbokwe Kelechi, and I Dike Ijeoma. Philip Model Capability to Estimate Infiltration for Solis of Aba , Abia State. 5(2):63–68, 2015.

[31] Giovanni Ravazzani, Chiara Corbari, Stefano Morella, Paride Gianoli, and Marco Mancini. Modified Hargreaves-Samani Equation for the Assessment of Reference Evapotranspiration in Alpine River Basins. *Journal of Irrigation and Drainage Engineering*, 138(7):592–599, 2012.

[32] Martin Allen, Richard G., PEREIRA, Luis S., RAES, Dirk and SMITH. FAO Irrigation and Drainage Paper Crop by. *Irrigation and Drainage*, 300(56):300, 1998.

[33] By George H Hargreaves. Defining and using reference evapotranspiration. *Journal of Irrigation and Drainage Engineering*, 120(6):1132–1139, 1994.

[34] Nicola Montaldo, Vania Toninelli, John D. Albertson, Marco Mancini, and Peter A. Troch. The effect of background hydrometeorological conditions on the sensitivity of evapotranspiration to model parameters: Analysis with measurements from an Italian alpine catchment. *Hydrology and Earth System Sciences*, 7(6):848–861, 2003.

[35] N. Montaldo, G. Ravazzani, and M. Mancini. On the prediction of the Toce alpine basin floods with distributed hydrologic models. *www.interscience.wiley.com*, 2274(November 2008):2267–2274, 2007.

[36] Daniela Osorio Zuluaga. 431 rayos en medellín, inundaciones y árboles caídos, balance del aguacero, 6 2021. `https://www.elcolombiano.com`.

[37] Daniela Osorio Zuluaga. Río medellín crecido e inundaciones viales: balance de las lluvias, 6 2021. `https://www.elcolombiano.com/antioquia/vias-inundadas-y-rio-medellin-crecido-por-lluvias-DC14165798`.

[38] National Oceanic and Atmospgeric Administration (NOAA). Global forecast system, 6 2021. `https://www.ncdc.noaa.gov/data-access/model-data/model-datasets/global-forcast-system-gfs`.

[39] National Oceanic and Atmospgeric Administration (NOAA). GFS, 6 2021. `HTTPS://WWW.EMC.NCEP.NOAA.GOV/EMC/PAGES/NUMERICAL_FORECAST_SYSTEMS/GFS.PHP`.

Appendix A

Maps of precipitation

This appendix reports the maps of daily cumulated precipitation in millimeters for the periods of time from 31 August 2020 to 05 August 2020 (*Event 1*) and from 27 November 2020 to 2 December 2020 (*Event 2*). Maps are generated at 3:00 a.m. so they refer to the previous day. These maps are reported to show the differences between forecast precipitation and the interpolated precipitation starting from measured data.

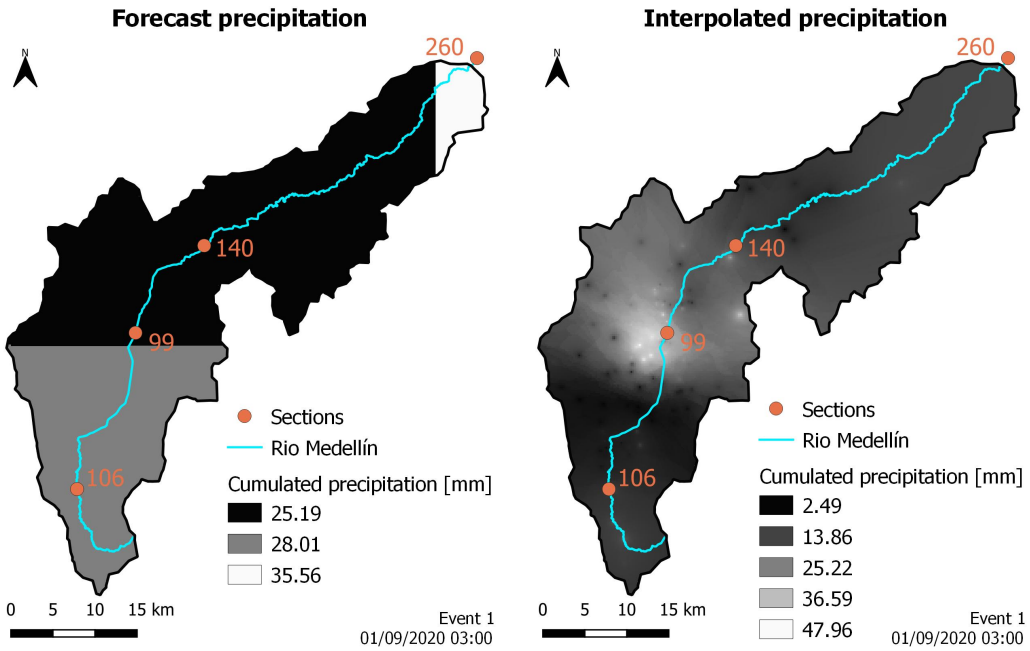

(a) (b)

Figure A.1: Maps of cumulated precipitation 01/09/2020 - Event 1

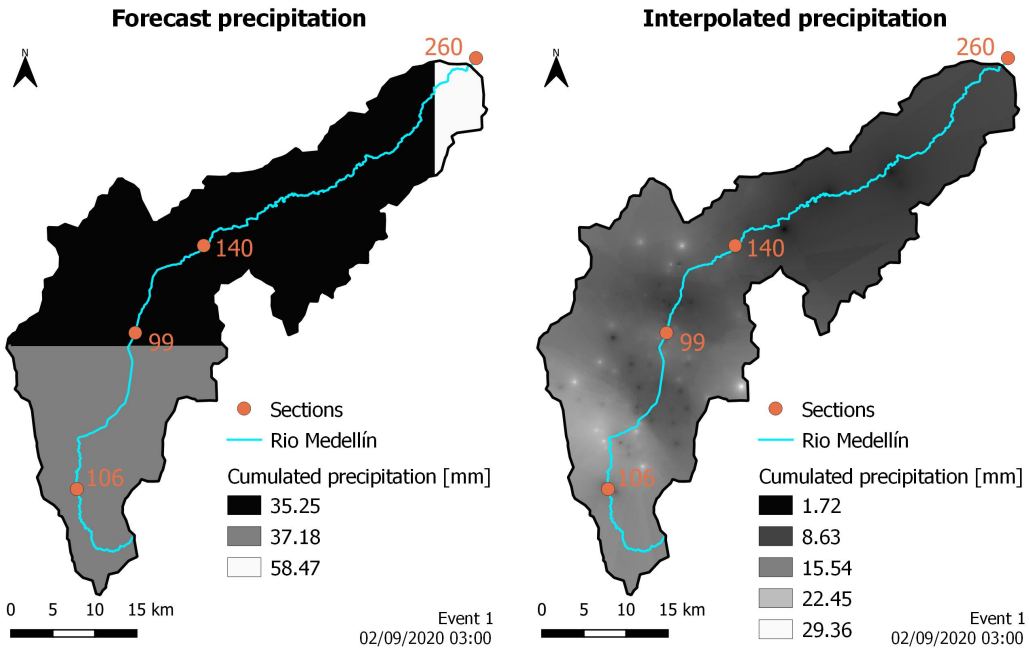

(a) (b)

Figure A.2: Maps of cumulated precipitation 02/09/2020 - Event 1

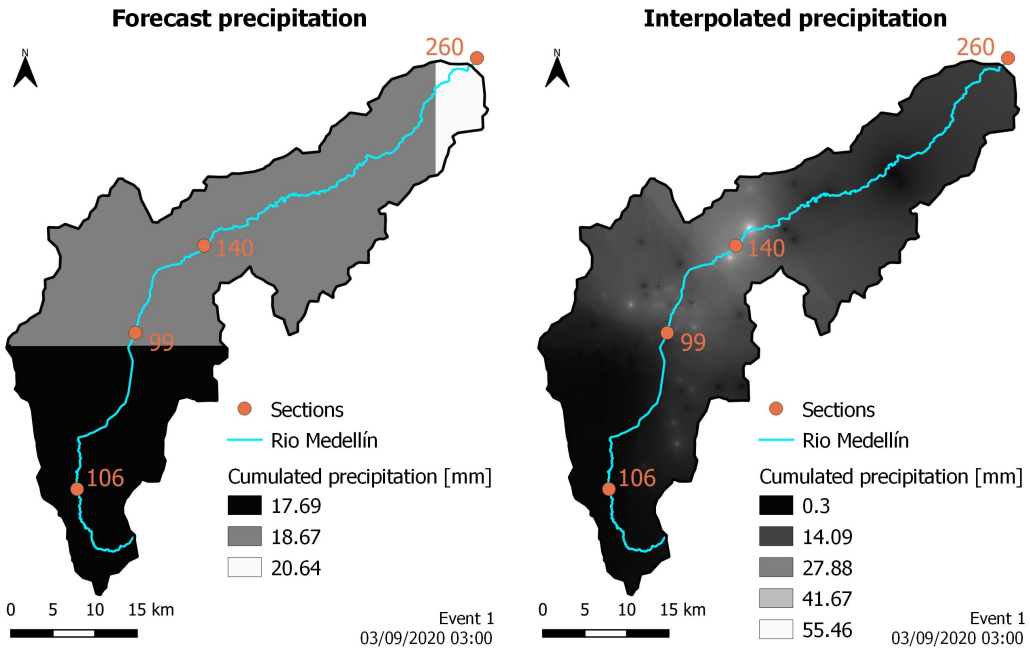

(a) (b)

Figure A.3: Maps of cumulated precipitation 03/09/2020 - Event 1

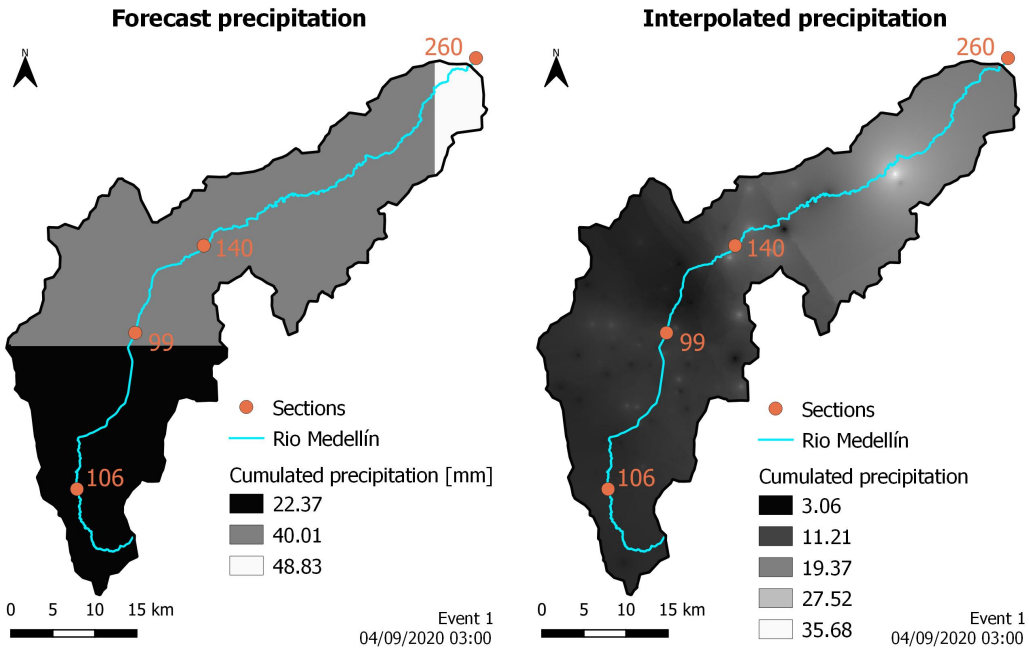

(a) (b)

Figure A.4: Maps of cumulated precipitation 04/09/2020 - Event 1

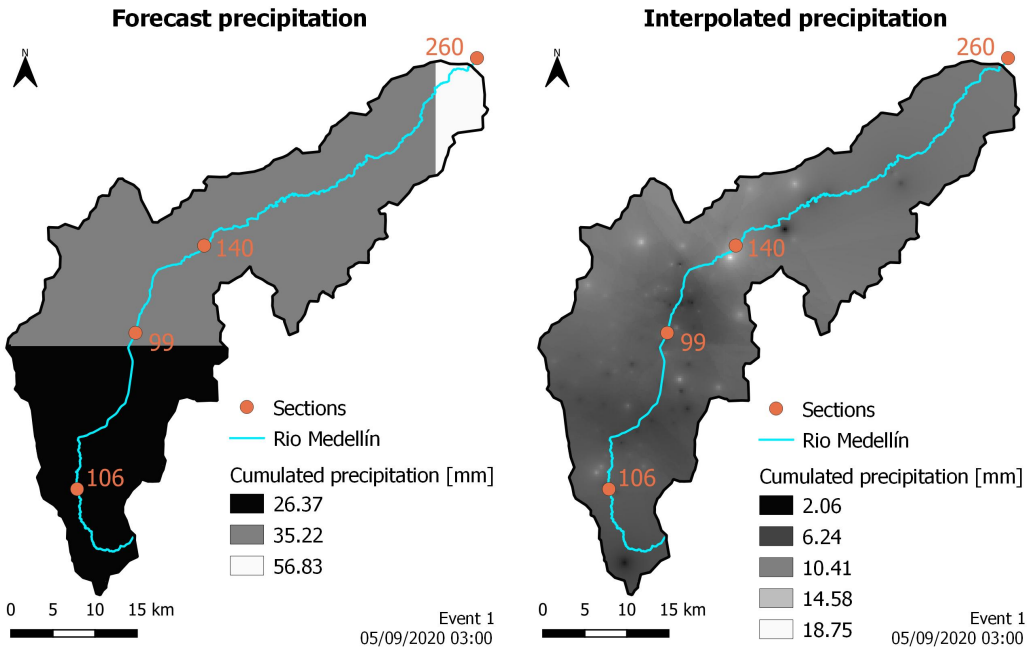

(a) (b)

Figure A.5: Maps of cumulated precipitation 05/09/2020 - Event 1

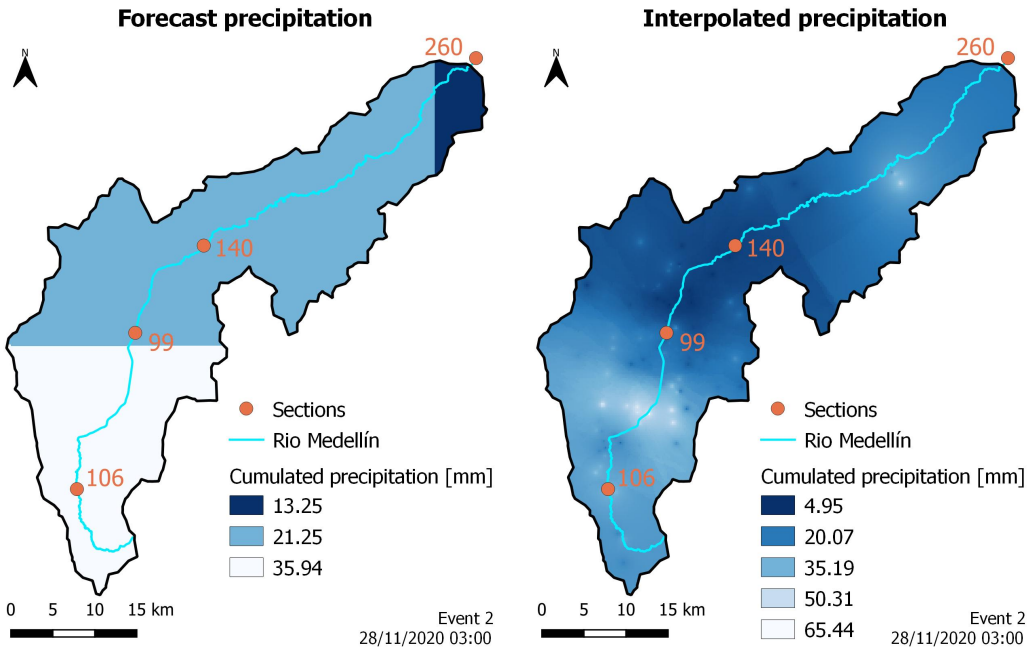

(a) (b)

Figure A.6: Maps of cumulated precipitation 28/11/2020 - Event 2

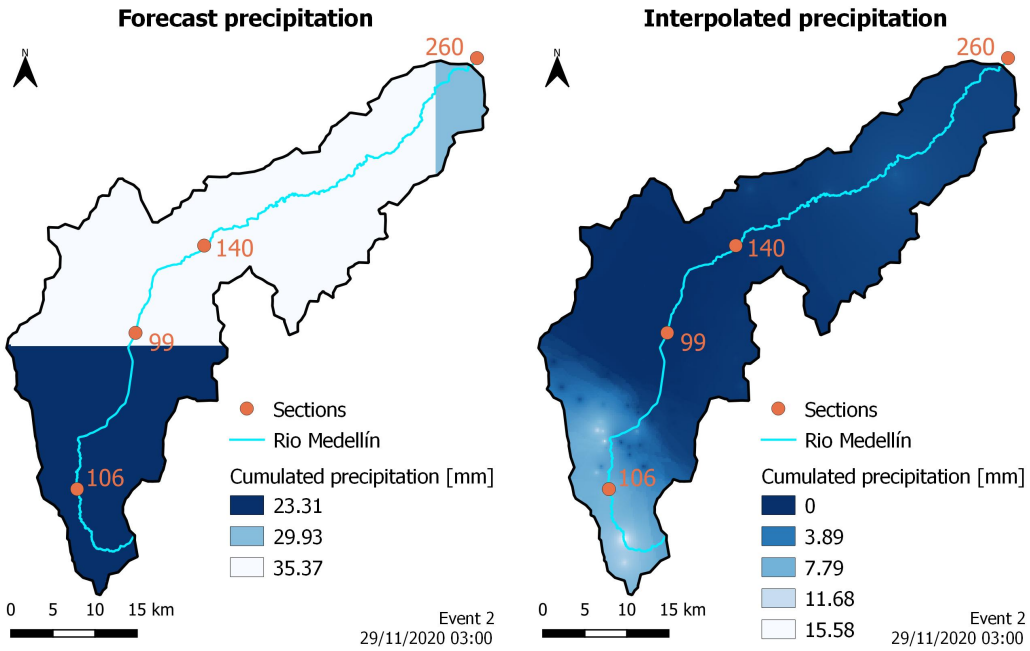

(a) (b)

Figure A.7: Maps of cumulated precipitation 29/11/2020 - Event 2

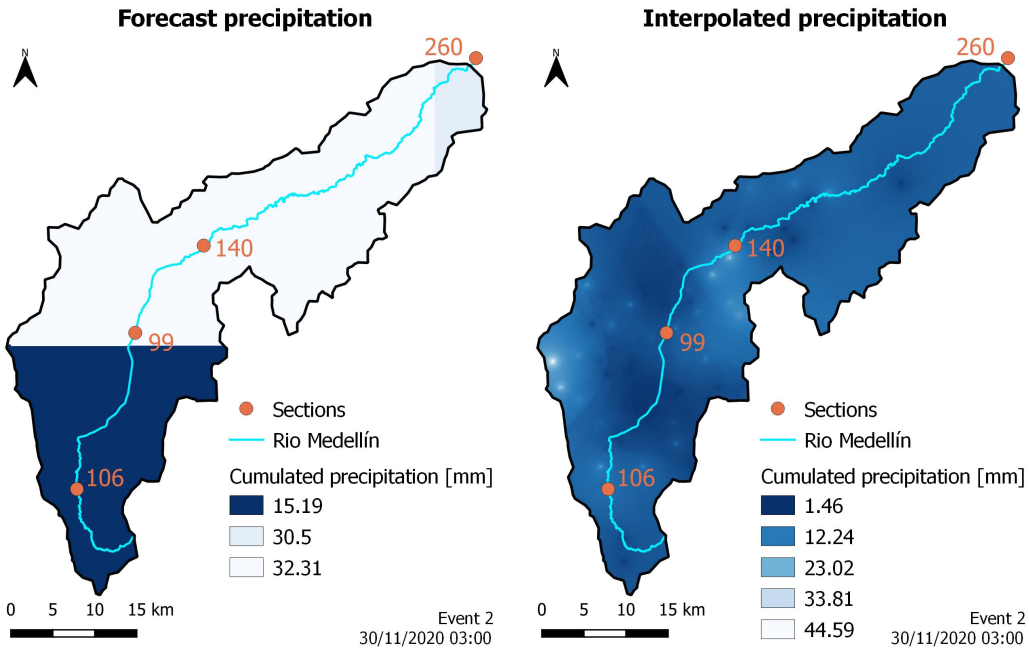

(a) (b)

Figure A.8: Maps of cumulated precipitation 30/11/2020 - Event 2

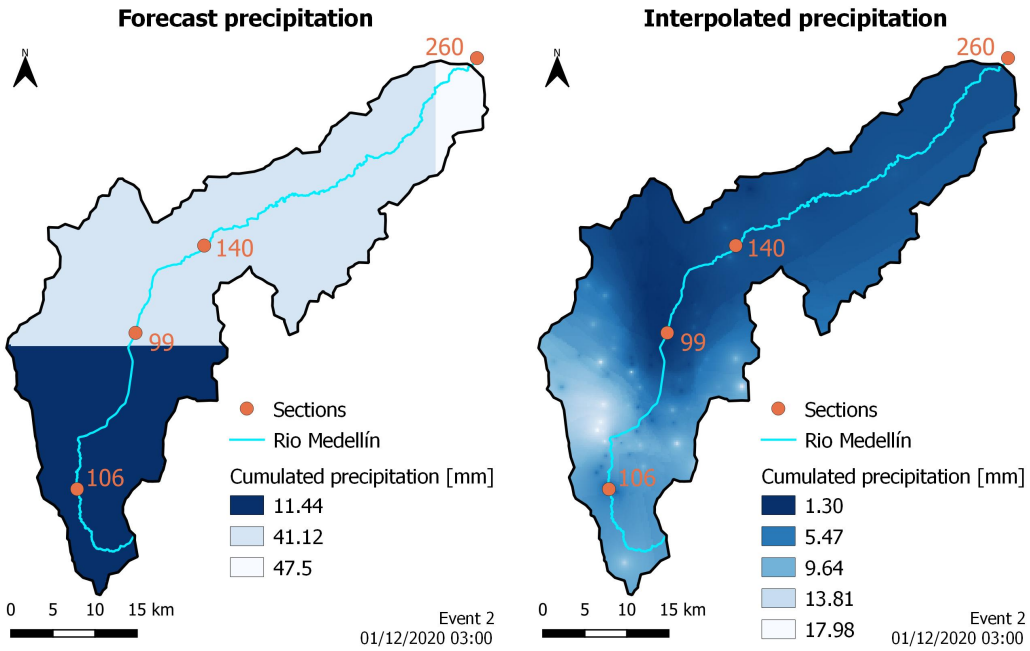

(a) (b)

Figure A.9: Maps of cumulated precipitation 01/12/2020 - Event 2

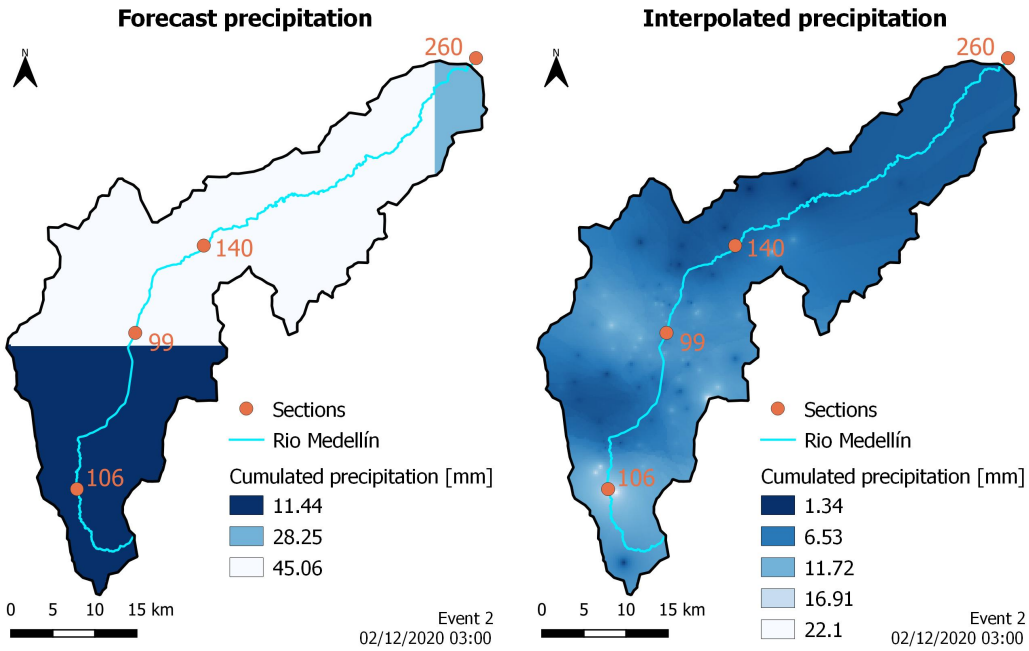

(a) (b)

Figure A.10: Maps of cumulated precipitation 02/12/2020 - Event 2

Appendix B

Rating curves

The appendix shows the graphs of the interpolation curve of water depth and discharge. In the table are also reported the coefficients a and b of the curve that is a power-law:

$$Q = ah^b \tag{B.1}$$

For the graph and the coefficient of the section of calibration (*3 Aguas*) see section 3.3 on page 32.

	Section	**a**	**b**
99	Aula Ambiental	7.13	3.53
140	Puente Fundadores Copacabana	17.14	1.45
260	Puente Gabino	0.07	4.36

Table B.1: Coefficients of the power-law

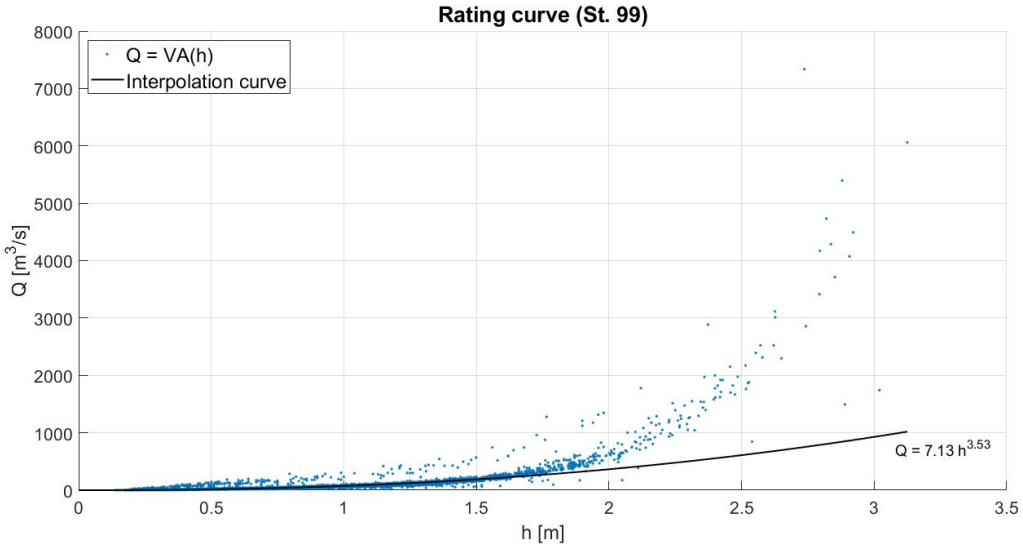

Figure B.1: Rating curve for the section Aula Ambeintal

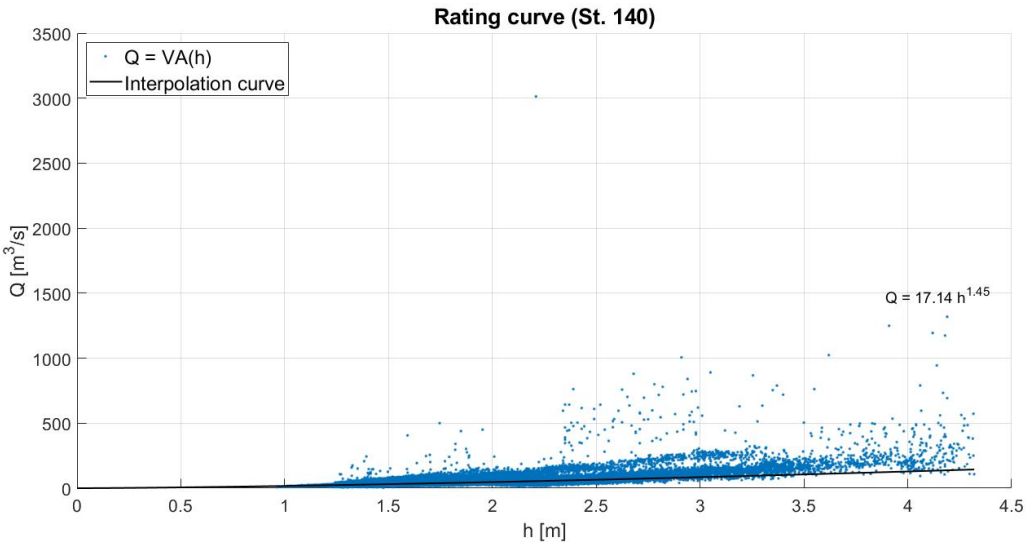

Figure B.2: Rating curve for the section Puente Fundadores Copacabana

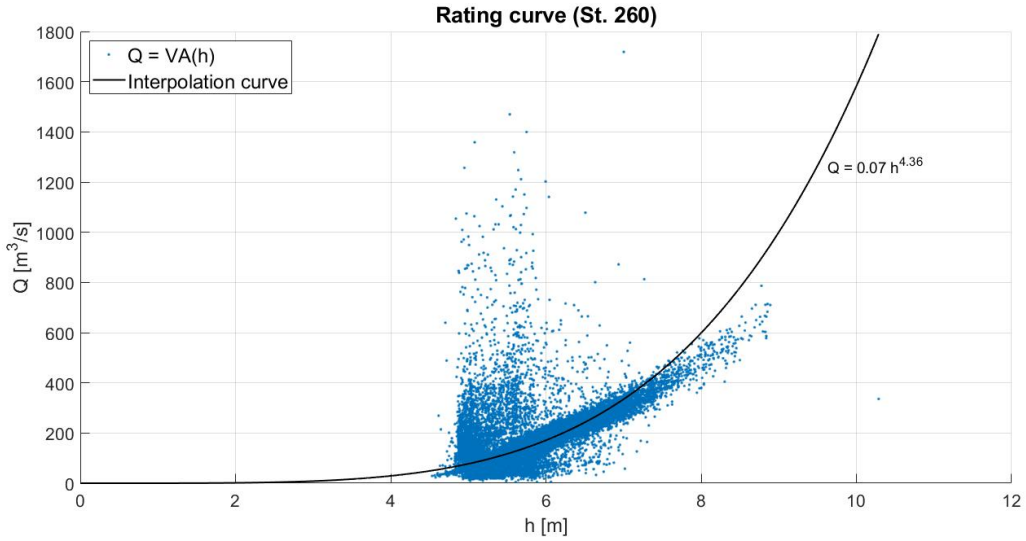

Figure B.3: Rating curve for the section Puente Gabino

Ringraziamenti

Desidero in primis ringraziare il Professor Giovanni Ravazzani che durante questi mesi, con calma e serenità, si è sempre reso disponibile sotto ogni punto di vista ed ha fatto in modo che io credessi sempre nelle mie capacità. Ringrazio inoltre Lisdey Verónica Herrera Gómez per il supporto fornito e soprattutto per la pazienza nel correggere la tesi.

Un enorme grazie va a Guglielmo che c'è stato fin dall'inizio. Mi ha sempre spronato, ascoltato e sopportato, grazie per aver sempre lasciato sfogare (su di te) le mie manie di controllo. Con lui perfino le sessioni d'esami diventavano accettabili. Senza di lui al poli mi sono sempre sentita un po' persa.
Non posso non ringraziare il Luca, fonte inesauribile di informazioni, un po' il nostro Barbero personale.
Ringrazio Fabio che ha reso tutto più giocoso e leggero strappandomi sempre un sorriso.
Ringrazio la Fede per tutte le sessioni di gossip, fondamentale per sopravvivere alle sessioni d'esami.
Infine vorrei ringraziare Irene, senza di lei quest'ultimo periodo sarebbe stato decisamente molto meno gestibile e molto più triste.

Desidero ringraziare i miei genitori per avermi sostenuto durante questo lungo percorso lasciandomi i miei tempi e miei spazi, ovviamente senza di loro non avrei concluso un bel niente.

"Siamo tutti un po' pazzi a volte"
B.L.